AD-A185 985 DETERMINATION OF CLOUD BASE HEIGHT AND EMISSIVITY FROM 1/1
DOWNWELLING ANGULAR RADIANCES(U) AIR FORCE INST OF TECH
WRIGHT-PATTERSON AFB OH J L SORLIN-DAVIS 1987
UNCLASSIFIED AFIT/CI/NR-87-93T F/G 4/2 NL

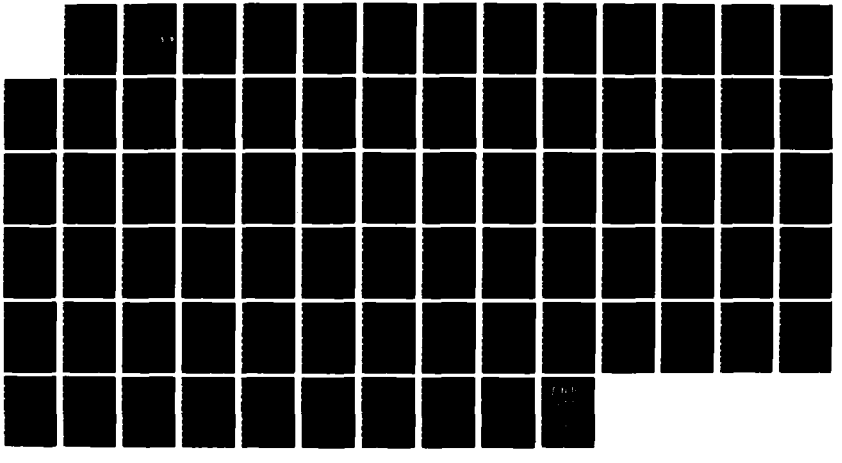

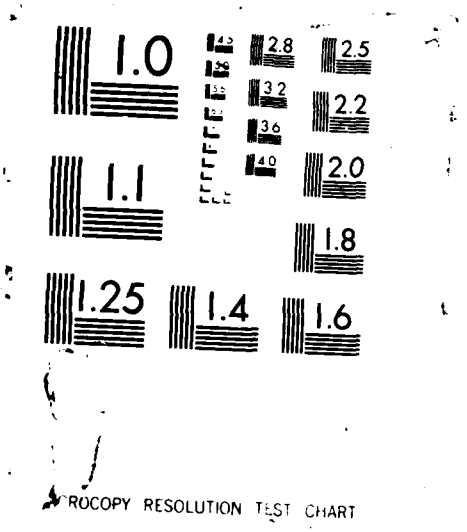
1.0
1.1
1.25
2.8
3.2
3.6
4.0
2.5
2.2
2.0
1.8
1.4
1.6
ROCOPY RESOLUTION TEST CHART

UNCLASSIFIED
SECURITY CLASSIFICATION OF THIS PAGE (When Data Entered)

REPORT DOCUMENTATION PAGE

READ INSTRUCTIONS BEFORE COMPLETING FORM

1. REPORT NUMBER: AFIT/CI/NR 87-93T	2. GOVT ACCESSION NO.
3. RECIPIENT'S CATALOG NUMBER	
4. TITLE (and Subtitle): Determination Of Cloud Base Height And Emissivity From Downwelling Angular Radiances	5. TYPE OF REPORT & PERIOD COVERED: THESIS/DISSERTATION
	6. PERFORMING ORG. REPORT NUMBER
7. AUTHOR(s): Janet Louise Sorlin-Davis	8. CONTRACT OR GRANT NUMBER(s)
9. PERFORMING ORGANIZATION NAME AND ADDRESS: AFIT STUDENT AT: Colorado State University	10. PROGRAM ELEMENT, PROJECT, TASK AREA & WORK UNIT NUMBERS
11. CONTROLLING OFFICE NAME AND ADDRESS: AFIT/NR, WPAFB OH 45433-6583	12. REPORT DATE: 1987
	13. NUMBER OF PAGES: 68
14. MONITORING AGENCY NAME & ADDRESS (if different from Controlling Office)	15. SECURITY CLASS. (of this report): UNCLASSIFIED
	15a. DECLASSIFICATION DOWNGRADING SCHEDULE

16. DISTRIBUTION STATEMENT (of this Report)

APPROVED FOR PUBLIC RELEASE; DISTRIBUTION UNLIMITED

17. DISTRIBUTION STATEMENT (of the abstract entered in Block 20, if different from Report)

18. SUPPLEMENTARY NOTES

APPROVED FOR PUBLIC RELEASE: IAW AFR 190-1

LYNN E. WOLAVER 23 Sept 87
Dean for Research and
Professional Development
AFIT/NR

19. KEY WORDS (Continue on reverse side if necessary and identify by block number)

20. ABSTRACT (Continue on reverse side if necessary and identify by block number)

ATTACHED

DD FORM 1 JAN 73 1473 EDITION OF 1 NOV 65 IS OBSOLETE

SECURITY CLASSIFICATION OF THIS PAGE (When Data Entered)

THESIS

DETERMINATION OF CLOUD BASE HEIGHT AND EMISSIVITY FROM DOWNWELLING ANGULAR RADIANCES

Submitted by

Janet Louise Sorlin-Davis

Atmospheric Science Department

In partial fulfillment of the requirements

for the Degree of Master of Science

Colorado State University

Fort Collins, Colorado

Summer, 1987

COLORADO STATE UNIVERSITY

May 6, 1987

WE HEREBY RECOMMEND THAT THE THESIS PREPARED UNDER OUR SUPERVISION

BY Janet L. Sorlin-Davis

ENTITLED Determination of Cloud Base Height and Emissivity from Downwelling Angular Radiances

BE ACCEPTED AS FULFILLING IN PART REQUIREMENTS FOR THE DEGREE OF

Master of Science .

Committee on Graduate Work

Adviser

Department Head

ABSTRACT OF THESIS

DETERMINATION OF CLOUD BASE HEIGHT

AND EMISSIVITY FROM DOWNWELLING ANGULAR RADIANCES

A technique has been devised which uses ground-based radiance observations to estimate the base height and spectral emissivity of a homogeneous cloud layer. From the spectral emissivity, a broadband emissivity can also be deduced. An error sensitivity analysis was performed to simulate the effects of instrument errors. Model calculations at 10μm and 11μm showed that homogeneous cloud layers produce unique sets of ground radiance values over a range of zenith angles from 0° to 90°. By examining downwelling ground radiances at a very small zenith angle and a second zenith angle between 40° and 80°, one can distinguish between low emissivity-low clouds and high emissivity-high clouds. This is possible because the cloud emissivity and the atmospheric transmissivity beneath a cloud are dependent on the viewing angle, thus affecting how much radiation reaches the ground; as a result, this relationship differs for every cloud height and emissivity.

Janet Louise Sorlin-Davis
Atmospheric Science Department
Colorado State University
Fort Collins, CO 80523
Summer 1987

ACKNOWLEDGEMENTS

The author wishes to express her appreciation to Dr. Stephen K. Cox for his guidance and support throughout the development of this research. This appreciation is also extended to Melissa Tucker for her patience and help with the word processing requirements, and to Judy Sorbie for her timely and talented drafting support.

This research was supported by the United States Air Force/Air Force Institute of Technology and by research grants from National Aeronautics and Space Administration, Grant Number NAO300 and Department of Defense-NAVY-Office of Naval Research, Grant Number DE0306.

TABLE OF CONTENTS

	Page
ABSTRACT	iii
ACKNOWLEDGEMENTS	iv
TABLE OF CONTENTS	v
LIST OF FIGURES	vii
I. INTRODUCTION	1
II. SPECTRAL INFRARED MODEL	5
A. Pre-modification	5
B. Modification for Clouds	8
III. CLOUD HEIGHT, EMISSIVITY, AND ANGULAR RADIANCE	16
A. Data Used	16
1. Wavelength	16
2. Clear-Sky Atmosphere	17
3. Cloud Cases	20
B. Results of Cloud Simulations	22
IV. APPLICATION OF TECHNIQUE	29
A. 10μm and 11μm Calculations	29
B. Iterative Solution for Cloud Height and Emissivity	36
1. Principles of Solution	37
2. Construction of Radiance Tables	37
3. Definition and Incorporation of Errors	41
4. Generation of Test Cases and Results	44

		Page
	C. Discussion of Results	52
	D. Broadband Emissivity	55
	E. Summary of Solution Procedure	59
V.	CONCLUSION	63
VI.	REFERENCES	67

LIST OF FIGURES

		Page
Fig. 1a.	Schematic definition of τ (upwelling case).	7
Fig. 1b.	Schematic definition of τ (downwelling case).	9
Fig. 2.	Schematic view of downwelling radiance components and new definition of τ and τ' for a homogeneous cloud case.	12
Fig. 3.	Skew-T representation of temperature/moisture profile used to define a clear-sky atmosphere. The temperature and dewpoint profiles are represented by the solid lines. The dashed line indicates values initially used for cloud dewpoints, when a cloud existed (see section III.A.3.).	18
Fig. 4.	Downwelling radiance curves as a function of zenith angle for 9 out of 21 cloud test cases (10μm).	23
Fig. 5a.	Atmospheric emission component as a function of zenith angle (10μm).	24
Fig. 5b.	Cloud emission component as a function of zenith angle (10μm).	25
Fig. 5c.	Above cloud transmission component as a function of zenith angle (10μm).	26
Fig. 6a.	Total downwelling radiance curves as a function of zenith angle for the 500mb and 600mb cloud cases (10μm).	30
Fig. 6b.	Cloud emission component as a function of zenith angle for the 500mb and 600mb cloud cases (10μm).	31
Fig. 7a.	Total downwelling radiance curves as a function of zenith angle for the 500mb and 600mb cloud cases (11μm).	33
Fig. 7b.	Cloud emission component as a function of zenith angle for the 500mb and 600mb cloud cases (11μm).	34

Page

Fig. 7c. Cloud emission component maxima between 40° and 90° for the 500mb and 600mb cloud cases (11μm). 35

Fig. 8. Example comparison of total downwelling radiance curves for variations in the precipitable water for three levels beneath a cloud base. 42

Fig. 9. Flowchart for program SEARCH. 46

Fig. 10. Spectral emissivity of clouds of various thicknesses vs wavenumber or wavelength, reproduced from Yamamoto, 1969. 56

Fig. 11. Broadband emissivity as a function of 10μm spectral emissivity for -36°C and +16°C cloud base temperatures. 58

Fig. 12a. Summary of model demonstration used to determine the height and emissivity of an unknown cloud layer. 60

Fig. 12b. Summary of major equations used in model demonstration. 61

I. INTRODUCTION

In recent years, the interest in radiative properties of a cloudy atmosphere has continued to grow. Of all possible atmospheric constituents, clouds have the greatest potential for altering the long and short term radiative budget. There is an ongoing attempt to incorporate complex cloud radiative processes into forecasting models, global and local energy studies, and satellite retrieval systems. Whereas clear sky radiation models have been developed with much success (Manabe and Strickler, 1964), the introduction of clouds into these models presents unique problems.

Most of the major longwave and shortwave radiation problems associated with clouds center around their highly variable reflecting, transmitting, and emitting properties. Each of these properties depends not only on microphysical characteristics of the cloud, i.e. cloud droplet size, distribution and shape, but also on cloud thickness and height. Although shortwave cloud reflectivity has become invaluable in satellite technology, infrared cloud characteristics are most important for heat budget studies of the atmosphere. Using a drop-size distribution scheme developed by Diem (1948), Yamamoto (1966, 1969) and Zdunkowski (1971) showed what effect the microphysical make-up and height of clouds had on infrared radiative models. They both determined that the reflectivity, emissivity and transmissivity of clouds were dependent on a cloud's prescribed physical characteristics and could not

be assumed constant. Zdunkowski, however, showed that reflectivity in the infrared changed little with cloud thickness while emissivity and transmissivity varied from near zero to 1.0. Reflectivity values rarely exceeded 10%. Therefore, although reflectivities could be assumed nearly constant and small, constant emissivity/transmissivity values could no longer be used for all cloud situations.

Actual radiation observations taken above and below clouds also revealed the highly variable emissivities and transmissivities of clouds. Allen (1970), using comparisons of infrared radiometric measurements for low, middle, and high clouds, determined that emissivities varied from 100% for low, thick clouds to an average of 35% for cirrus clouds. Experimental measurements gathered by Paltridge (1974) led to conclusions that even low stratoform clouds can have emissivities much less than 100%. Paltridge found that drop size radii for these clouds averaged less than originally suggested by Diem, thus leading to smaller emissivity calculations. Platt (1972, 1977) combined lidar, radiometer, and satellite observations and showed that cirrus clouds had emissivities that varied from near zero to 100%. He found that variations in emissivities were not strictly related to cloud thickness, even when the microphysics of a cloud were thought to be uniform. Griffith and Cox (1979) used aircraft and radiometric data to define a broadband mass absorption coefficient for tropical cirrus clouds which was used to relate emissivities to ice/liquid water content and thicknesses of clouds. Whereas some previous theoretical studies had predicted cirrus emissivities of less than 1.0 for a 6 km thick cloud, Griffith and Cox found emissivities near 1.0 for cirrus which was only 1-1.2 km thick.

During the past two decades, the majority of cloud emissivity and transmissivity studies were and are directed towards cirrus clouds because of their questionable effect on global climate (Cox, 1971 and Fleming and Cox, 1974). However, variable radiative properties of lower clouds should not be ignored. Cox (1975) used 300 radiometersonde ascents in a midlatitude and tropical region and showed emissivities for clouds between the surface and 300mb all averaged significantly below 100%. The highest average downward effective emissivities were not recorded for low clouds, as might be expected, but were recorded for clouds between 400 and 600mb. This was thought to be related to the mean water vapor mass distribution with height. Davies (1985) also showed average cloud emissivities to be 68, 58 and 22% for low, middle and high clouds, respectively. Although low, warm water clouds have been easier to study and understand in terms of physical structure and formation, these findings support further radiation research for clouds at heights other than cirrus levels.

The primary purpose of this research project was to devise and assess a technique which might be used to develop a climatology of radiation with regards to cloud emissivity and cloud height. Downwelling radiance was of primary interest because it is the component observable from the ground and can be viewed at different zenith angles. Most experiments of the past concentrated only on a 0° viewing angle in order to simplify calculations and observations. Yamamoto and Tanaka (1969) related model calculations of total emergent radiation from a cloud to its angular distribution, but this relationship was limited to only one specific cloud case. They were mainly interested in how

radiation observed at the base of a cloud changed as a function of angle for different wavelengths and for different cloud thicknesses.

This research, however, explored how ground-based radiances over several viewing angles might be used to distinguish between homogeneous cloud layers with different heights and emissivities. The angular differences in model-calculated ground radiances provided information which was used to make this distinction. If only one viewing angle had been considered, many cloud configurations could have explained the single observed radiance at that angle; a low cloud with a low emissivity could result in the same radiance measurement as a higher cloud with a high emissivity. But the rate of change of downwelling radiance from a 0° to 90° viewing angle appeared to differ significantly for different clouds. By examining this angular change in radiance, this study showed that the base height and emissivity of an unknown cloud layer can possibly be estimated by observing ground-based radiances at more than one zenith angle.

II. SPECTRAL INFRARED RADIATION MODEL

In order to show that angular radiative measurements can provide information on cloud heights, two steps were followed. First of all, a spectral infrared radiative transfer model called RADLON, described by Cox, et al., (1976), was modified to incorporate clouds which could vary in height and emissivity. For a given cloud layer, the base height and physical properties were uniform, but the emissivity derived from these parameters was modified into a function of viewing angle. Secondly, once the model was modified to include clouds, multiple simulations were run for clouds of different heights and emissivities. These simulations were compared to show that angular downwelling radiance values between 0 and 90° could be used to determine a unique cloud base height.

A. Pre-modification

RADLON was chosen for this cloud study because of its versatility in radiance calculations. Using RADLON, radiance computations can be made for a specific wavelength or for a range of wavelengths, for one atmospheric level or for several. The user prescribes the pressure levels into which the atmosphere is to be divided along with the atmospheric temperature and gas profiles. The water vapor mixing ratio (g/kg), carbon dioxide mixing ratio (g/kg), and ozone mixing ratio (μg/g) can all be varied by the user, although carbon dioxide, in this case, was assumed constant at 330 ppm by volume or .501 g/kg (Liou,

1980). Absorption data has been built into the model according to several sources (Cox, 1976) and includes the water vapor continuum absorption region (8-12 μm) as prescribed by Bignell (1973).

RADLON was also initially designed to simulate only clear sky radiative transfer processes. Under this clear sky assumption, RADLON's calculation of terrestrial radiation reaching the top of the atmosphere was based on two components: radiation emitted by a blackbody surface (usually the ground, but this could be a cloud top) and transmitted up through the atmosphere in wavelengths where atmospheric absorption is weak, plus radiation that is emitted by the atmosphere in wavelengths where atmospheric gaseous absorption/emission is strong. The integral equation used to express this total upwelling radiance is (Coulson, 1975):

$$N\uparrow(\nu,\tau,+\mu)=B(\nu,\tau,+\mu)e^{-(\tau_1-\tau)/\mu}+\int_{\tau_1}^{\tau} J(\nu,t)e^{-(t-\tau)/\mu}\,dt/\mu \qquad (1)$$

where τ is the optical thickness, defined in Figure 1a, B is the Planck function, ν is the wavenumber, μ is the cosine of the zenith angle (θ), t is a dummy integration variable for τ, $N\uparrow$ is the upwelling radiance, and J is the atmospheric source term. $N\uparrow$ is in units of $Wm^{-2}sr^{-1}/10cm^{-1}$. The $10cm^{-1}$ is necessary because radiance calculations are actually made for a $5cm^{-1}$ wavenumber interval on either side of the specified wavenumber. The first term on the RHS of the equation represents the attenuated surface emitted radiation, and the second term represents the attenuated atmospheric emitted radiation integrated through all levels.

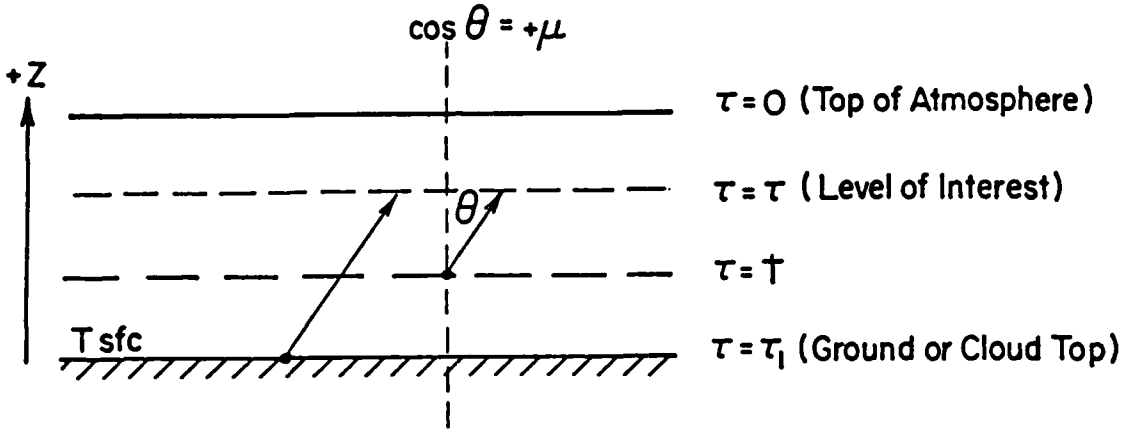

Fig. 1a. Schematic definition of τ (upwelling case).

The surface emission term was based entirely on blackbody assumptions. Assuming blackbody properties only, initial surface and atmospheric emission was computed using (Liou, 1980)

$$B_\nu(T) = 2h\nu^3/c^2[\exp((h\nu/KT)-1)] \qquad (2)$$

where $B_\nu(T)$ is the temperature dependent Planck function, h is Planck's constant, ν is the wavenumber, c is the speed of light, and K is Boltzman's constant. During the integration process, the average temperature of a given layer was determined from the assumed temperature/pressure profile.

For downwelling radiances ($N\downarrow$), the first term on the RHS of equation 1 can be omitted since the corresponding temperature at the top of the atmosphere is near absolute zero, and the resultant Planck function approaches zero. Therefore, for clear sky conditions, downwelling terrestrial radiation reaching a surface is due mainly to the emission of the atmospheric gases, H_2O vapor, CO_2, and O_3, and is represented by a similar integral equation:

$$N\downarrow(\nu,\tau,-\mu) = \int_{\tau_0}^{\tau} J(\nu,t)e^{(t-\tau)/\mu}\, dt/\mu \qquad (3)$$

where $N\downarrow$ is the downwelling radiance, and τ is now defined by Figure 1b.

B. Modification for clouds

In order to study the effects of clouds on downwelling radiance at the ground or at any level in the atmosphere, equation 3 was modified to account for the radiative effects of a given cloud layer. In the simplified case where a cloud is assumed to be a blackbody emitter, only a surface emitting term similar to that in equation 1 would be needed.

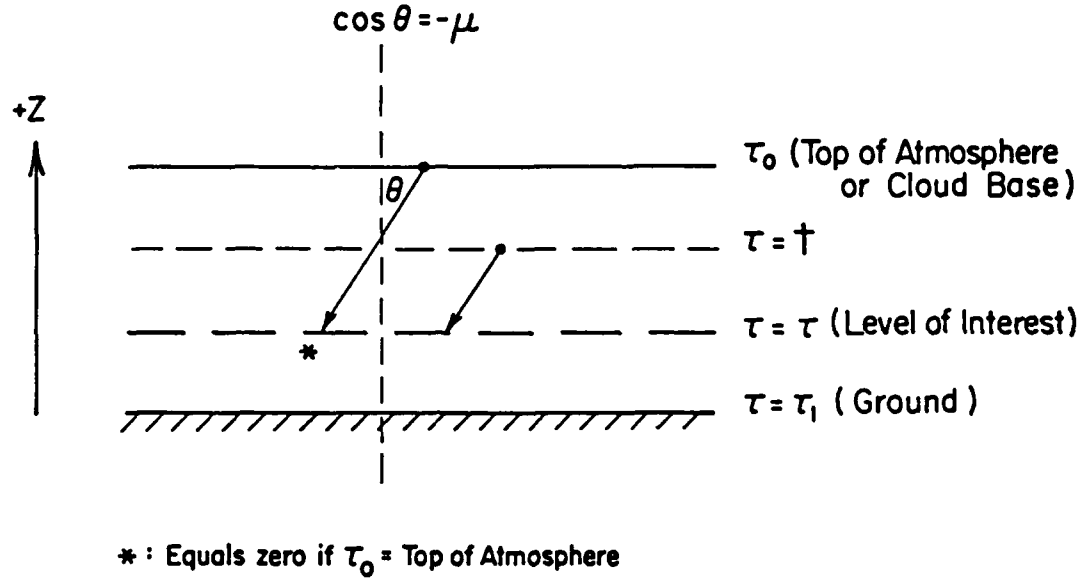

Fig. 1b. Schematic definition of τ (downwelling case).

However, clouds cannot always be considered blackbodies so their emissivities (therefore, transmissivities) must be allowed to vary under different conditions. For instance, thin or low water content clouds have lower emissivities than thick, high water content clouds. For clouds with emissivities less than 100%, three terms must be included in the downwelling radiance equation. Radiation originating from above, below, and from the cloud itself must be taken into consideration. The radiative transfer equation for a single layer, grey body cloud case then becomes:

$$N\downarrow(\nu,\tau,-\mu) = A + B + C \qquad (4)$$

where:

$$A = \int_{\tau_B}^{\tau_1} J(\nu,t)e^{(t-\tau_1)/\mu}\, dt/\mu$$

$$B = \{(\varepsilon_\nu)B(\nu,T_{cloud})\}\, e^{(\tau_B-\tau_1)/\mu}$$

$$C = \{[(1-\varepsilon_\nu)\int_{\tau_0}^{\tau_T} J(\nu,t)e^{(t'-\tau_T)/\mu}\, dt/\mu]\}\, e^{(\tau_B-\tau_1)/\mu}\ .$$

where T_{cloud} is the average temperature of a cloud, ε_ν is the spectral emissivity of the cloud, and $1-\varepsilon_\nu$ is the spectral transmissivity. Clouds were assumed to be isothermal, and T_{cloud} was set equal to the temperature at the base of the cloud. The spectral emissivity will be referred to simply as "emissivity" for the remainder of this paper, which differs from the broadband emissivity. The spectral emissivity relates to one particular wavelength whereas the broadband emissivity relates to an average emissivity over a range of wavelengths. Further on in this paper, a simple model will be used to calculate a broadband emissivity from a derived spectral emissivity.

For simplicity, reflectivity has been assumed negligible, i.e. the sum of the emissivity and transmissivity of a cloud is equal to one. For infrared wavelengths, this is not an unreasonable assumption (Zdunkowski, 1971). Term A in equation 4 represents the atmospheric radiative contribution below the cloud, term B represents the effective grey body cloud emission, and the C term represents the cloud top incident radiation which is transmitted through the cloud. This last term is based on clear sky radiance calculations for the pressure level of an assumed cloud top. This incident radiation is multiplied by the cloud transmissivity and then attenuated by the intervening atmosphere between the cloud base and the ground. Figure 2 shows a schematic view of the three components of the total downwelling surface radiance for any angle θ and the new defintion of τ and τ'.

As shown in equation 4, if the emissivity of a cloud can vary, then downwelling radiance calculations at a particular angle can also vary, depending on which term of the equation dominates. Small changes in a cloud's emissivity could actually result in significant changes in radiances observed at the ground, especially for low, warm clouds. Therefore, being able to accurately evaluate a cloud's emissivity has become an important challenge for modern research.

The emissivity of a cloud is normally thought of as a function of the physical characteristics of the cloud, i.e. the liquid/ice water content and the thickness. For example, Griffith(1979) proposed that a cloud's emissivity could be determined from:

$$\varepsilon_{cloud} = 1-\exp(-K \cdot LWC \cdot \Delta Z) \qquad (5)$$

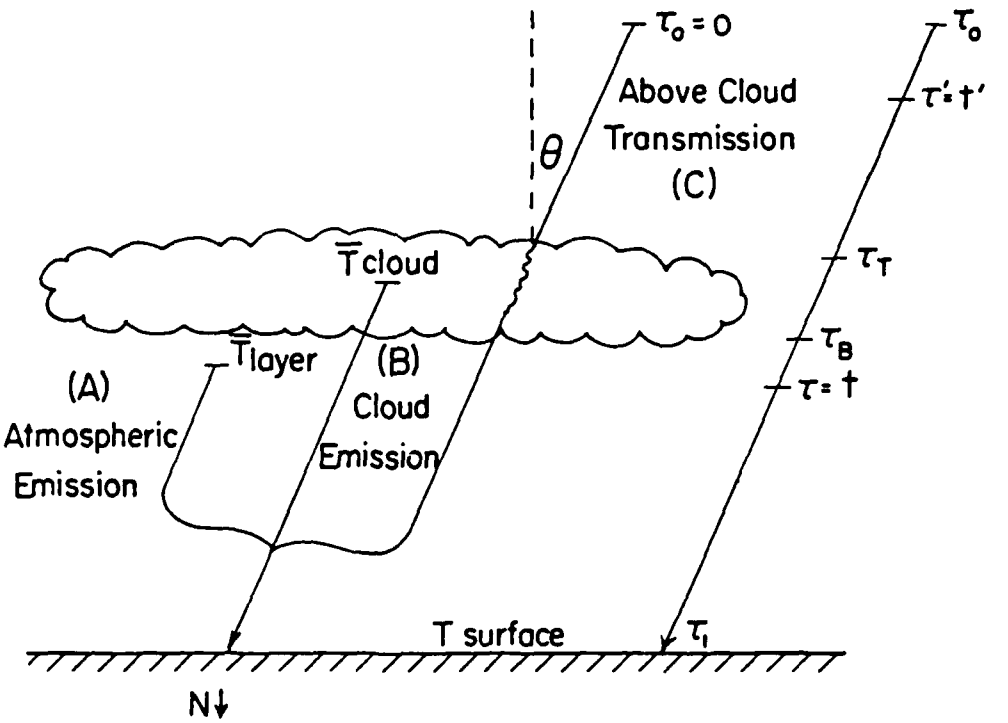

Fig. 2. Schematic view of downwelling radiance components and new definition of τ and τ' for a homogeneous cloud case. A, B, and C refer to terms in equation 4.

where K is an empirically derived mass absorption coefficient, LWC is the ice or liquid water content of the cloud, and ΔZ is the thickness of the cloud. Equation 5 was based on previous emissivity studies by Paltridge(1974) and experimental data collected by Griffith. The exponent in the equation is related to the optical depth of the cloud. This type of relationship, however, is important mainly for studies concerned with how the physical structure of a cloud affect emissivity. For the research presented in this paper, the concern was not so much on what determined a cloud's emissivity but what effect a particular emissivity had on altering radiation received at the ground.

The viewing angle dependency of equation 5 is normally accounted for by allowing the effective liquid water mass to vary linearly with $\sec\theta$, thus replacing $LWC \cdot \Delta Z$ with $LWC \cdot \sec\theta \cdot \Delta Z$. RADLON was modified to account for the dependence of a cloud's emissivity on viewing angle according to the following set of equations:

$$\varepsilon_o = 1. - \exp(-K \cdot LWC \cdot \Delta Z \cdot \sec 0°) \qquad (6)$$

$$\text{or} \quad \ln(1. - \varepsilon_o) = -K \cdot LWC \cdot \Delta Z = -\text{const}$$

$$\varepsilon_\theta = 1. - \exp(-\text{const} \cdot \sec\theta) \qquad (7)$$

$$\text{or} \quad \varepsilon_\theta = 1. - \exp[\ln((1. - \varepsilon_o)^{\sec\theta})]$$

$$\text{or} \quad \varepsilon_\theta = 1. - (1. - \varepsilon_o)^{\sec\theta}$$

where ε_o is the zero degree zenith angle emissivity, ε_θ is the angular dependent emissivity, and $(1. - \varepsilon_o)$ equals the zero degree transmissivity of the cloud. Equation 6 is simply a general form of equation 5, and equation 7 accounts for the angular dependence of a cloud's emissivity.

For a given cloud, if ε_o is known, "const" can be calculated, and ε_θ can be determined for any angle. Equation 7 shows that as the zenith angle approaches 90°, the emissivity of a cloud approaches 100%, as would be expected if looking through an infinitely thick cloud. With this additional modification in RADLON, incremental changes in ε_o for different clouds could be controlled. Resultant changes in downwelling radiance at the ground could then be compared.

Once RADLON had been modified to account for any greybody cloud layer, model simulations could be made for clouds at several levels for any emissivity. Changes in downwelling radiances at the ground were compared for the same cloud(changing the emissivity) and for different clouds - all over a range of zenith angles. A separate clear sky model run was used to retrieve radiances that would be incident on cloud tops. These radiances were incorporated into a subroutine to allow them to vary as a function of angle while a cloud's transmissivity also changed as a function of the same angle. An important point to keep in mind is that the radiation incident on a cloud's top was assumed constant for all emissivities. At first this did not seem realistic, since equation 5 showed that emissivity can depend on cloud thickness. However, using equation 5, several model calculations were initially made which only varied the thickness of a cloud. Assuming the base height stayed the same, when the thickness of a cloud was changed, the radiation incident on the cloud top was also changed. K and LWC were held constant at $.0008m^{-1}$ (Griffith,1979) and ΔZ was changed from 500m to 1000m to 1500m, which related to 0° emissivities of .33, .55 and .77, respectively. These initial calculations with different cloud top incident radiances showed that taking thickness into account had little or no affect on

ground radiances, especially at large angles. From 0° to 90°, the decrease in a cloud's transmissivity with increasing angle significantly reduced any radiative contributions from above the cloud. Therefore, assuming constant values for cloud top incident radiation for a given cloud is justified.

By multiplying the cloud top incident radiance by the cloud's transmissivity, the radiation transmitted through the cloud from above was determined. The radiation emitted by the cloud (it's Planck Function based on its average temperature multiplied by emissivity) was then added to give the total radiation initiating at the base of the cloud. What part of this reaches the ground was dependent on the transmissivity of the atmosphere below the cloud. This transmissivity was also dependent on the zenith angle. The final radiance at the ground became a complex combination of the unattenuated cloud-related radiation plus the attenuated emission from the atmosphere below the cloud. Depending on the height of the cloud and zenith angle in question, each of these components would contribute differently to the total observed downwelling radiance. By studying downwelling radiances at different angles for different cloud cases, a relationship between cloud height, emissivity and angular radiances was determined. In the next section, the specific methodology for arriving at this relationship will be discussed. Following this qualitative discussion, a quantitative example will be used to show that an unknown cloud base height and spectral emissivity can be approximated by simple measurements of downwelling radiances over more than one viewing angle. A broadband emissivity can then be inferred from knowing the spectral emissivity for a single wavelength.

III. CLOUD HEIGHT, EMISSIVITY, AND ANGULAR RADIANCE RELATIONSHIP

Investigating the relationship between downwelling radiances at several angles and greybody cloud heights required multiple cloud simulations with RADLON. Initially, radiances were calculated with known cloud emissivities and height. The microphysics and thicknesses were assumed constant. Changes in angular radiances for individual simulations were compared to each other and to the assumed clear-sky condition. These comparisons showed a clear relationship between radiances calculated between zenith angles of 0° and 90° and each unique cloud height and emissivity. This first section will show how this relationship was determined. The second section will demonstrate how this relationship can be used in practical applications to approximate cloud heights and emissivities strictly from ground radiances measured at two different angles.

A. Data Used

1. Wavelength

All initial downwelling radiance calculations were made using a wavelength of 10μm, which is in the atmospheric window region. In this region, the atmosphere is relatively transparent so that changes in cloud and atmospheric radiation can be observed at the ground. Conclusions derived from using this wavelength were then extended to 11μm to see if quantitative analyses of radiance were more useful with

one than the other. The dimer H_2O molecule and ozone are both important absorbers at 10μm, but ozone effects were minimal except in calculating downwelling radiation incident on cloud tops. Ozone concentrations below 300 mb are negligible, therefore contributing little to radiative processes below any tropospheric cloud used in the simulations. Using 11μm eliminated any effects of ozone and reduced complications associated with radiative processes above a cloud. Although carbon dioxide is prespecified in the initial gas profiles, its absorption is negligible at both 10μm and 11μm and doesn't enter into the radiance calculations.

2. Clear-sky Atmosphere

Prior to looking at the effects of clouds on downwelling radiance at the ground, an initial atmospheric profile was used to simulate a clear-sky situation. This provided data for radiation incident on a specific cloud top for angles between 0° and 90°. Downwelling radiance calculations were made for the ground as well as up to 36 levels of the atmosphere, depending on how finely the atmosphere needed to be divided. If a cloud's emissivity relied primarily on thickness, the atmosphere was divided into more levels to get radiance data for smaller increments of pressure change. This gave incident radiation data for cloud tops within a few millibars of each other. Figure 3 shows a skew-T representation of the temperature and moisture profile (mixing ratio was converted to dew point temperatures) used to define the clear-sky atmosphere. This particular profile was based on mid-latitude climatological temperature, moisture, ozone and carbon dioxide data assembled from several sources. Table 1 shows the data used, where W

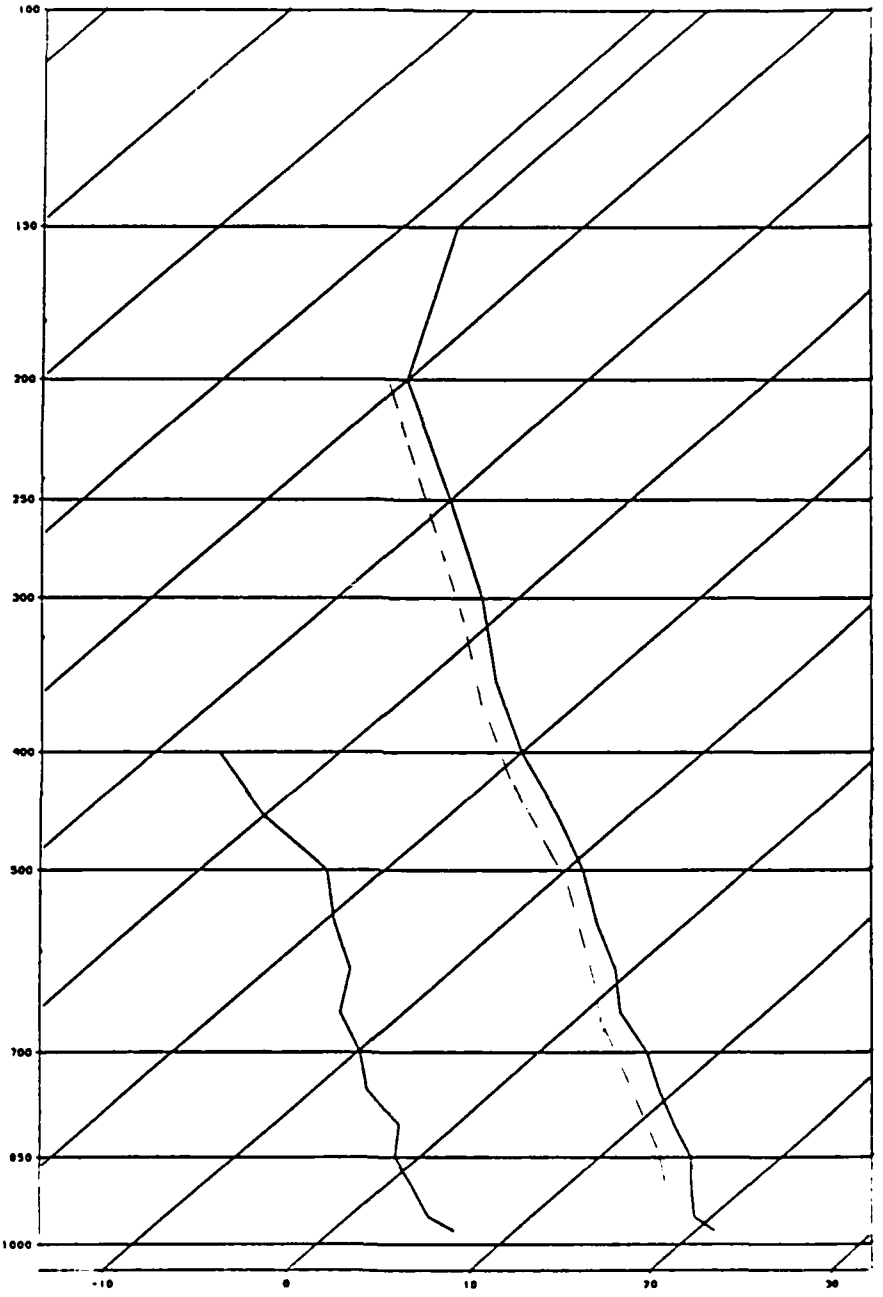

Fig. 3. Skew-T representation of temperature/moisture profile used to define a clear-sky atmosphere. The temperature and dewpoint profiles are represented by the solid lines. The dashed line indicates values initially used for cloud dewpoints, when a cloud existed (see section III.A.3.).

TABLE 1

Climatology Data for Standard Atmosphere

Pressure(mb)	W_{H2O}(g/kg)	W_{O3}(ug/g)	W_{CO2}(g/kg)	Temp(°C)
975	6.3	0	.501	21
950	5.5	0	.501	19
900	4.8	0	.501	17
850	4.1	0	.501	15
800	3.8	0	.501	12
750	3.0	0	.501	9
700	2.6	0	.501	6
650	2.1	0	.501	2
600	1.9	0	.501	-1
550	1.5	0	.501	-5
500	1.2	0	.501	-9
450	.7	0	.501	-14
400	.42	.1	.501	-20
350	.27	.2	.501	-26
300	.045	.2	.501	-32
250	.030	.5	.501	-40
200	.014	.8	.501	-50
150	.005	.8	.501	-57
100	.004	1.5	.501	-57
50	.003 (.006)	5.0	.501	-53
25	.003 (.017)	10.0	.501	-47
10	.003 (.020)	12.0	.501	-35
5	.003 (.018)	15.0	.501	-23
1	.003 (.014)	6.0	.501	-5

represents mixing ratio. Linear interpolation was used if more pressure levels were needed. The 975mb to 250mb data were taken from The Handbook of Geophysics and Space Environments (AFGL, 1965). The 200mb to 1mb data were taken from McClatchey (1972) to avoid extensive interpolation from the AFGL graphs. However, the 50mb to 1mb W_{H2O} values were set to .003 because RADLON could not make calculations for increasing moisture values at those levels (reason unknown). The mixing ratio values in parentheses indicate the unused McClatchey data.

3. Cloud Cases

Once clear-sky radiances had been calculated for zenith angles from 0-90°, cloud layers were then inserted. For each cloud case, the emissivity at 0° was preset and varied as a function of zenith angle, (equations 6 and 7). An attempt was made to initially choose 0° emissivities that could perhaps relate to specific thicknesses, even though it was determined that thickness really was not an important factor in this study. Since some calculations had already been made for emissivities of .33, .55, and .70 (corresponding to thicknesses of 500m, 1000m, and 1500m), these same emissivities were chosen to represent low, medium, and high emissivities for each cloud case. These emissivities correspond to ε_ν in equation 4. The radiation incident on the top of the cloud was taken from standard atmospheric calculations for the level of the cloud base, since changes in cloud top incident radiation were determined insignificant through 1500m.

The above two radiative contributions from the cloud and from above the cloud were predetermined and served as boundary conditions to the radiative transfer calculation of radiance at the earth's surface. The

initial temperature and gas profiles for each cloud case needed only to consist of data from the cloud base to the ground. In other words, for each individual cloud the only change made to the clear-sky profile was to omit all levels above the specified cloud base and increase the H_2O mixing ratio for the base level to make the moisture profile more realistic. The dashed line on Figure 3 shows an example of the simple cloud moisture profile used in the simulations. This moisture profile was arbitrarily chosen, but calculations done with several moisture changes at cloud level produced only slight changes at the surface (on the order of .1%). For the second part of this study, this moisture adjustment was eliminated for simplicity.

Individual cloud layer studies were chosen for low, middle, and high clouds. Each individual case was incorporated into RADLON to calculate downwelling radiance at the ground for more than one angle. The ground was at 975mb, and cloud base levels used were 900, 800, 700, 600, 500, 400 and 300mb. Each of these seven cases were given the three different 0° emissivities, i.e. .33, .55, .70. Therefore, there were a total of 21 individual simulations, each with downwelling radiance computations for angles between 0° and 90°. Radiances were computed for 5.07°, 22.50°, 39.93°, 50.07°, 67.5°, and 84.93°. These six angles correlate to weighted quadrature angles which are calculated internally by the model. No matter what the specified zenith angle range, there were always six quadrature angles with a similar type of weighting. These case studies provided the data base for determining whether or not there existed a well-defined relationship between radiances measured at different angles and the height of a cloud for any emissivity.

B. Results of Cloud Simulations

Figure 4 shows downwelling radiances at 10μm as a function of viewing angle for 9 of the 21 cloud cases. All cases exhibited similar patterns, but only the 900mb, 700mb, and 500mb cases are shown for clarity. Cloud cases with emissivities of .70 are represented by solid lines. Those with emissivities of .55 are represented by long dashed lines, and the short dashed curves represent cloud cases with emissivities of .33. As expected, low clouds with high emissivities produced the most dramatic increase in downwelling radiances at all angles. All curves eventually converged near $.899 Wm^{-2}sr^{-1}/10cm^{-1}$, which corresponds to the Planck function associated with the average temperature of the lowest layer of the atmosphere. The "standard" curve shows the downwelling radiance calculations for the clear-sky case. The most notable observation from this graph is the uniqueness of every curve. Also, none of the curves that represent the same cloud base and none of the curves that represent the same emissivity have any overlap. Overlapping curves only exist for clouds that differ in height and emissivity. The degree at which a particular curve changes slope from 0° to 90° appears to be most significant. Clouds that may result in similar radiance observations at small angles don't have similar radiances at larger angles. These differences in radiances observed at small and large angles are the first clue to relating cloud height and emissivity to radiances.

In order to find which angles may provide the most useful information for identifying clouds, the total radiance curves of figure 4 were divided into three separate components, as in equation 4. Figures 5a, 5b, and 5c represent the radiance contributions of the three

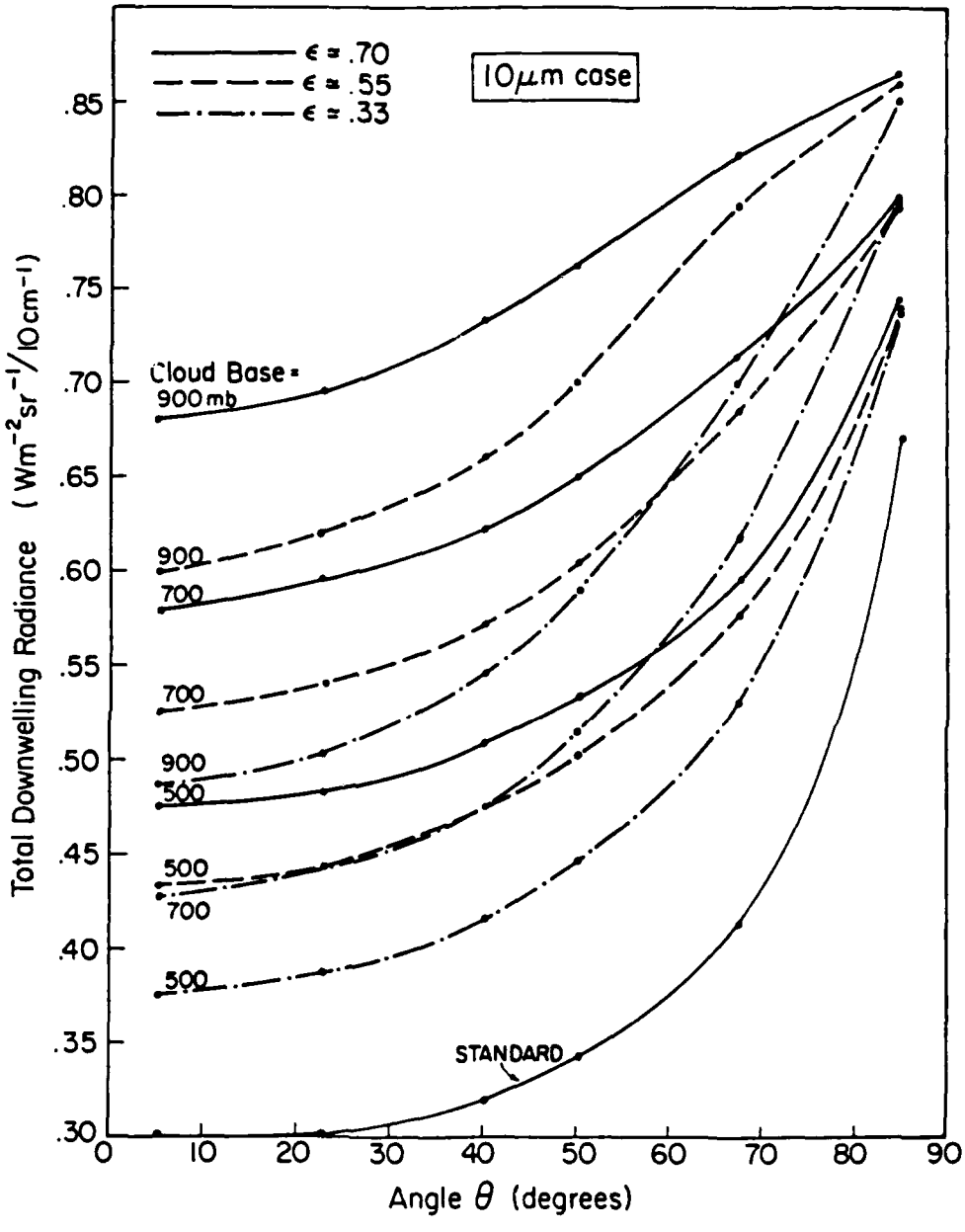

Fig. 4. Downwelling radiance curves as a function of zenith angle for 9 out of 21 cloud test cases (10μm).

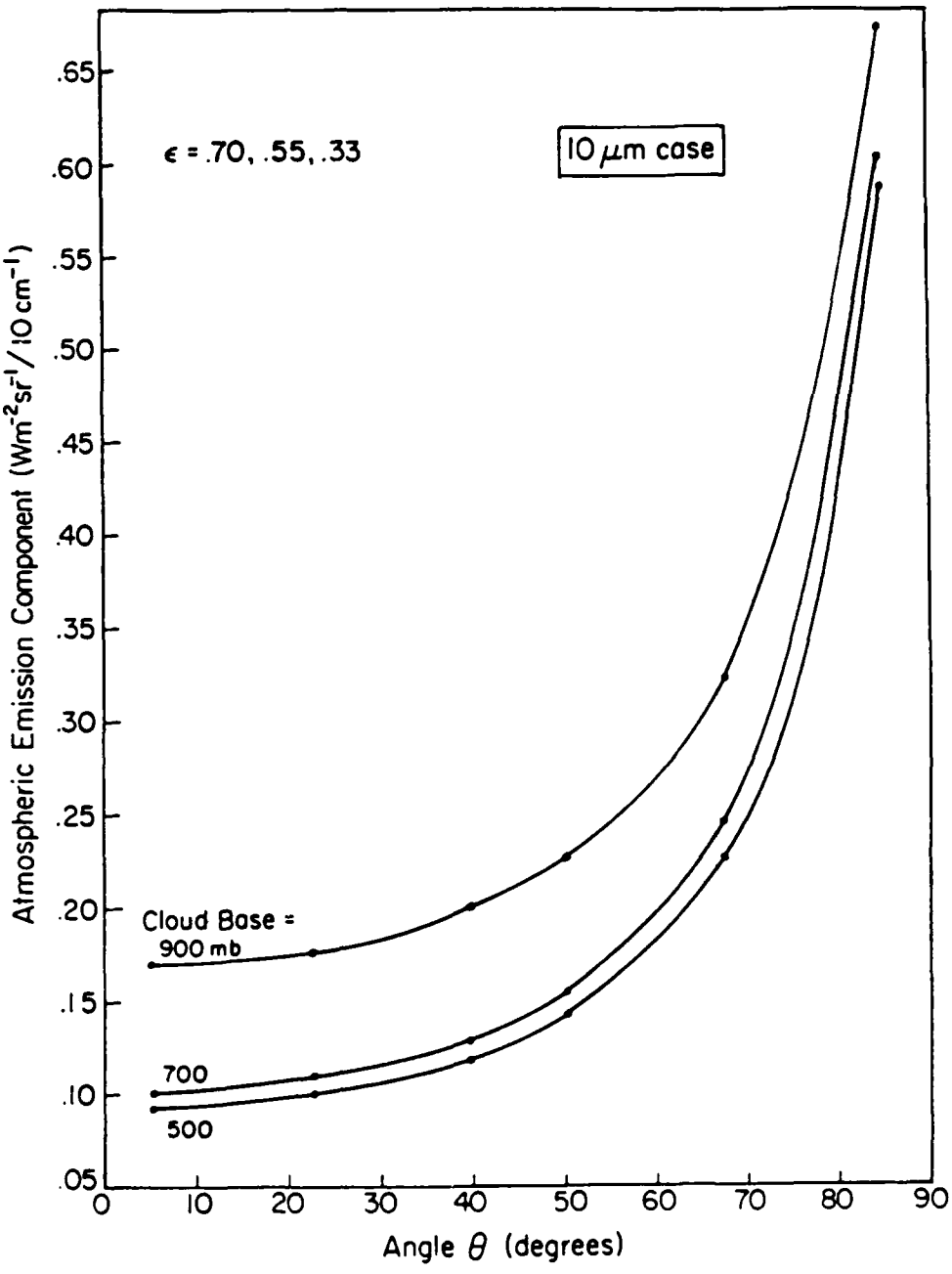

Fig. 5a. Atmospheric emission component as a function of zenith angle (10μm).

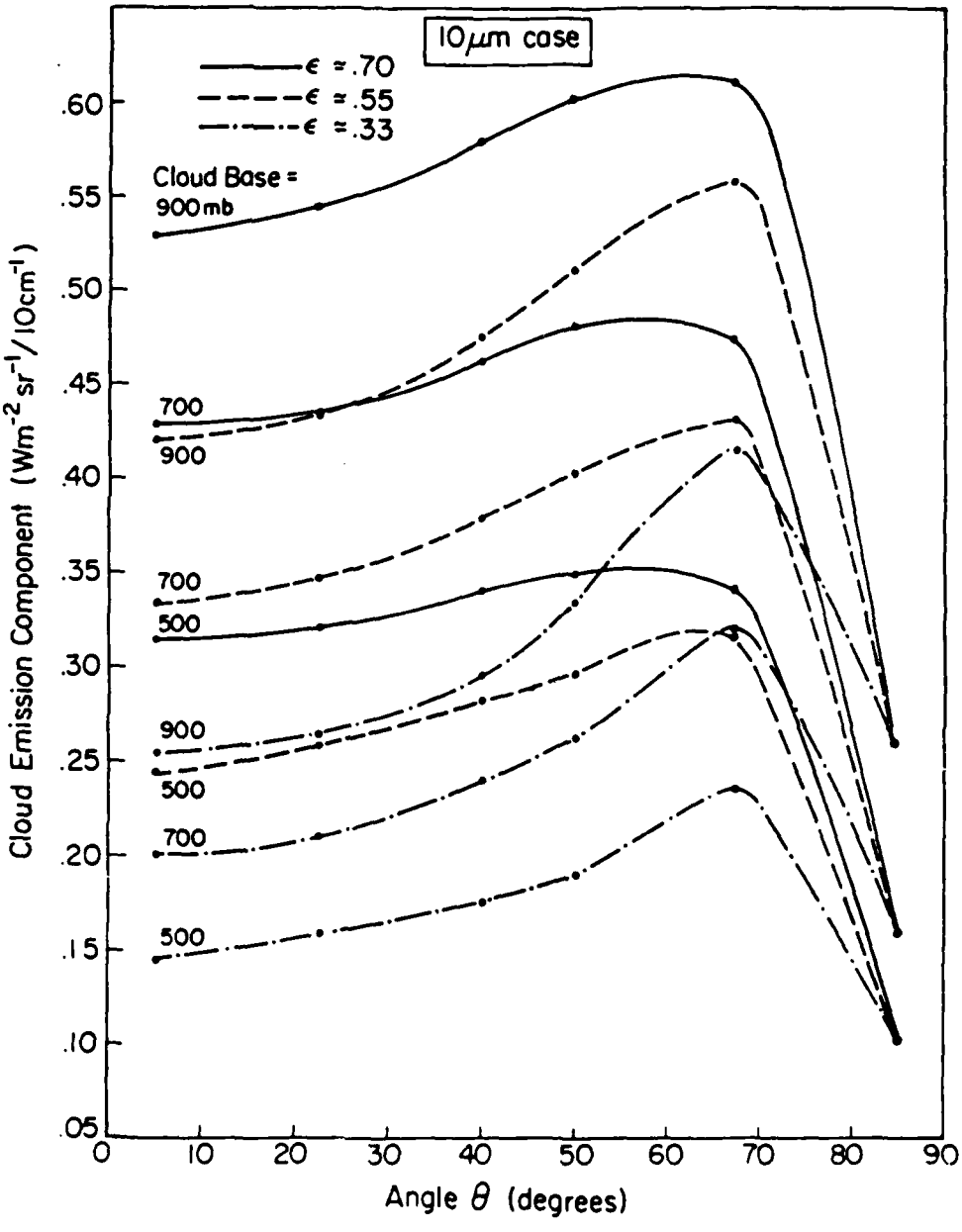

Fig. 5b. Cloud emission component as a function of zenith angle (10μm).

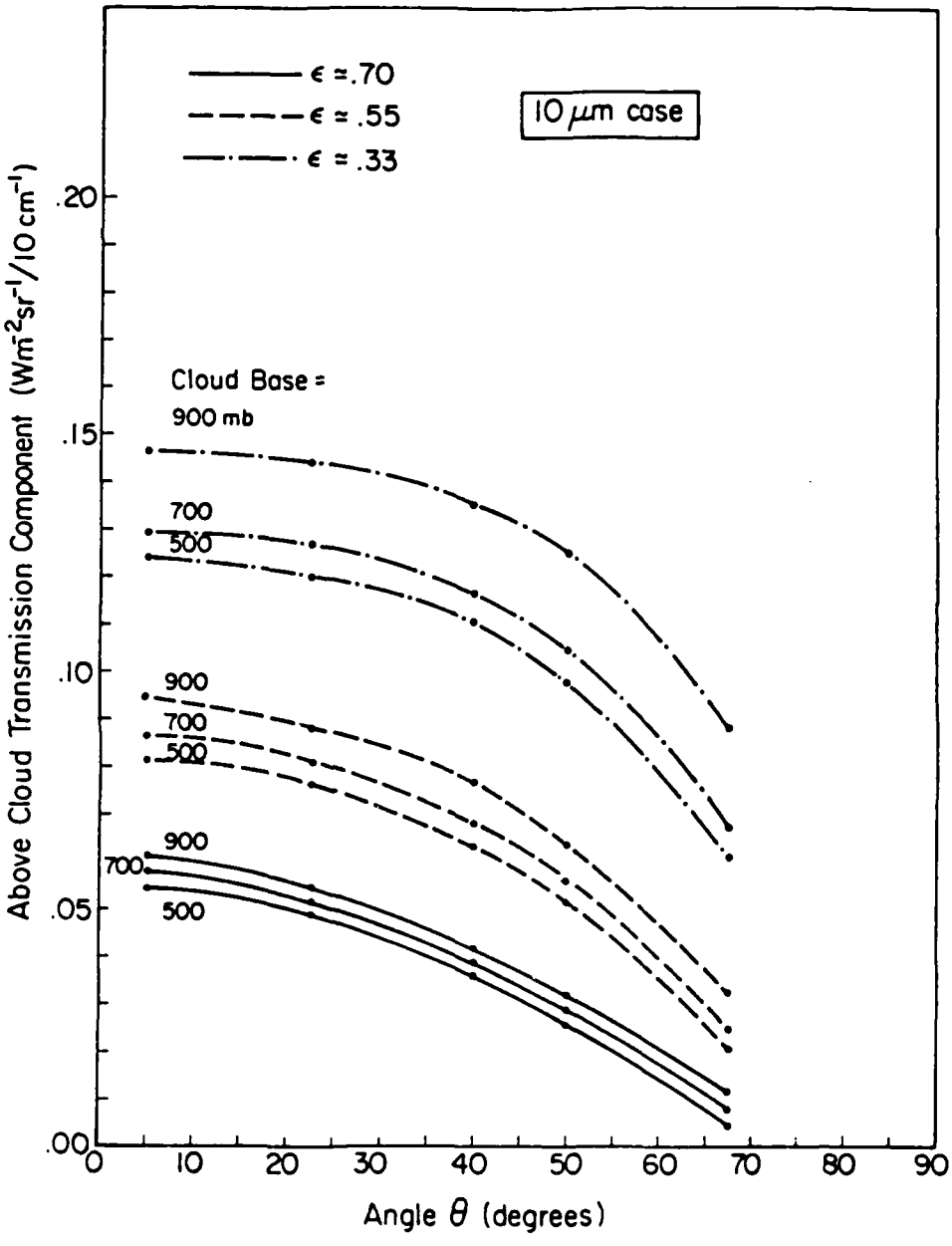

Fig. 5c. Above cloud transmission component as a function of zenith angle (10μm).

components; atmospheric emission, cloud emission, and cloud transmission, respectively. Figures 5a and 5c show little change in slope for individual curves. Figure 5b, however, shows significant peaking between the 40° and 80° zenith angles and significant overlap between different clouds with different emissivities. This cloud emission component appears to be primarily responsible for the uniqueness of curves in figure 4. This parallels the suggestion originally made by Yamamoto and Tanaka (1969). Through experimental observation, they had determined that emitted radiation from a cloud's base increases non-linearly with zenith angle. Their study encompassed the infrared region from 5-50μm but concentrated on 5.0μm and 6.3μm wavelengths. These were appropriate for observations directly beneath a cloud, but atmospheric absorption between the cloud and the ground is still significantly strong at these wavelengths. Changes in cloud emitted radiation would have little effect on radiation reaching the ground.

The atmosphere, however, is nearly transparent to wavelengths within the window region(8-12μm). Changes in cloud emitted radiation at these wavelengths would cause significant changes in the total radiation observable at the ground. According to Figure 5b, the angular increase in cloud emitted radiation that reaches the ground eventually becomes overshadowed by the angular exponential decrease in atmospheric transmissivity beneath the cloud. At angles between 40° to 80°, the cloud emission component still dominates over atmospheric attenuation, but drops off rapidly by 90°. The angle where cloud emission is most dominant depends on the amount of atmosphere beneath the cloud (how high is the cloud) and the 0° zenith angle emissivity. The lower the cloud

and the lower the emissivity, the larger the angle where a maximum in cloud emission is reached. In other words, the 900mb cloud with an emissivity of .33 shows a cloud emission peak at the largest angle, and the 300 mb cloud with an emissivity of .70 peaks at the smallest angle out of the 21 cases. Low emissivity clouds must be viewed through the larger angles to approach blackbody properties, and low clouds have less atmosphere below them to enhance attenuation. Since radiances were only computed at six specific angles, each precise cloud emission peak is difficult to determine, but appear to range from 40° to 70° for high to low clouds, respectively. In the next section, a more exact depiction of cloud emission maxima between 40° and 80° will be shown for an 11μm case study.

IV. APPLICATION OF TECHNIQUE

In the previous section, a relationship between greybody clouds and angular radiances was proposed. In order to determine the practical worth of this relationship, specific examples of clouds and radiances were examined to see if observed angular radiances could be used to identify the height of a cloud and its spectral emissivity. From these two parameters, a broadband emissivity for 5-50μm could also be deduced. The number of radiance curves, such as those in figure 4, that could be generated for all possible cloud situations, is infinite. Therefore, the following investigation concentrated on a relatively small section of the atmosphere between 500mb and 600mb. Conclusions made from studying this small section were assumed to pertain to the remainder of the atmosphere. In other words, if the height and emissivity of a cloud could be found within a small atmospheric section, then clouds at any atmospheric level could be identified using a similar procedure.

A. 10μm and 11μm Calculations

Figures 6a and 6b isolate the 500mb and 600mb cases from Figure 4 and Figure 5b, which were based on 10μm calculations. By magnifying this region, an analysis of radiance trends from 0° to 90° is more easily achieved. Figure 6a shows a good example of how two different clouds with the same 0° zenith angle radiance produce significantly different radiances at larger angles. The 600mb case with an emissivity

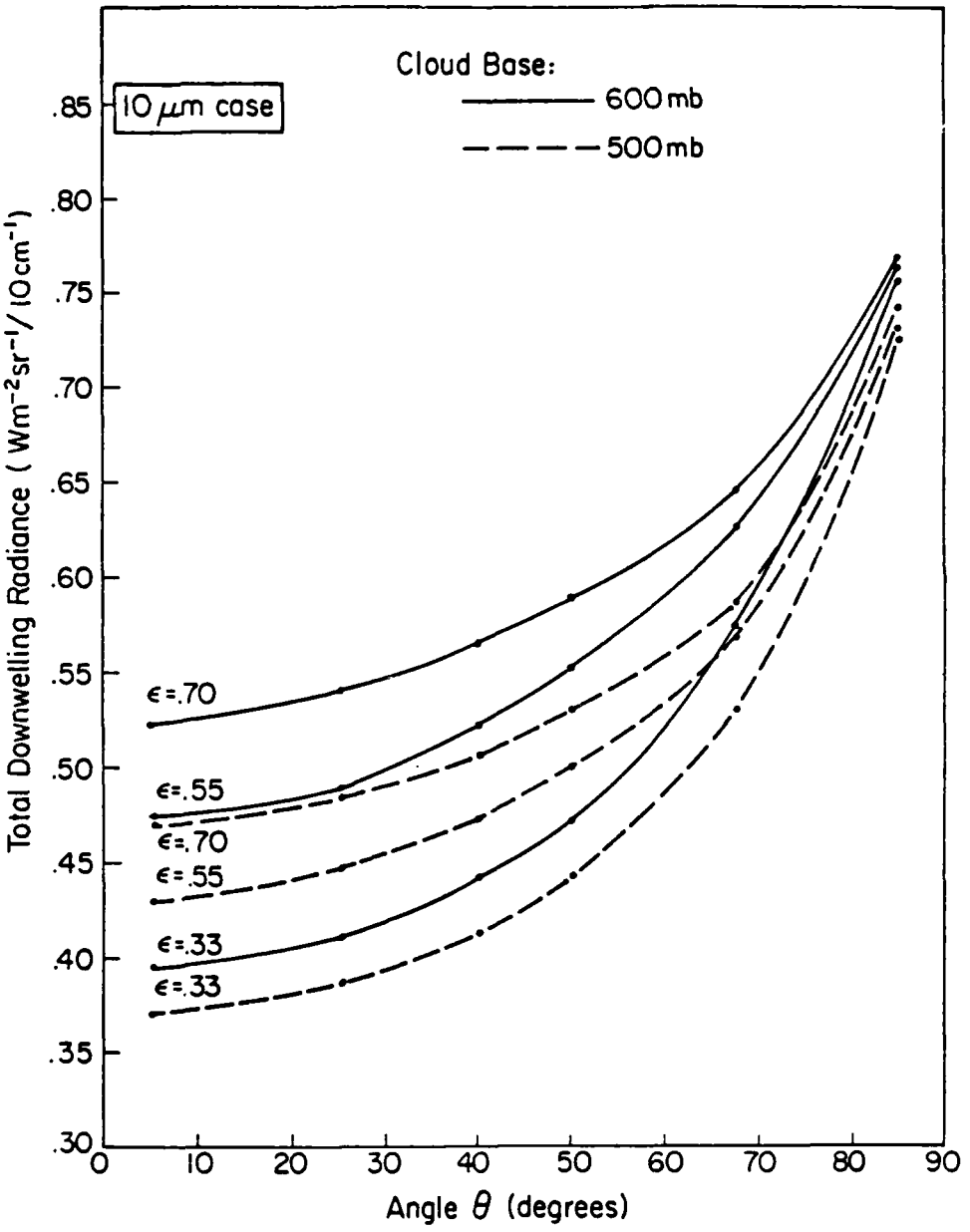

Fig. 6a. Total downwelling radiance curves as a function of zenith angle for the 500mb and 600mb cloud cases (10μm).

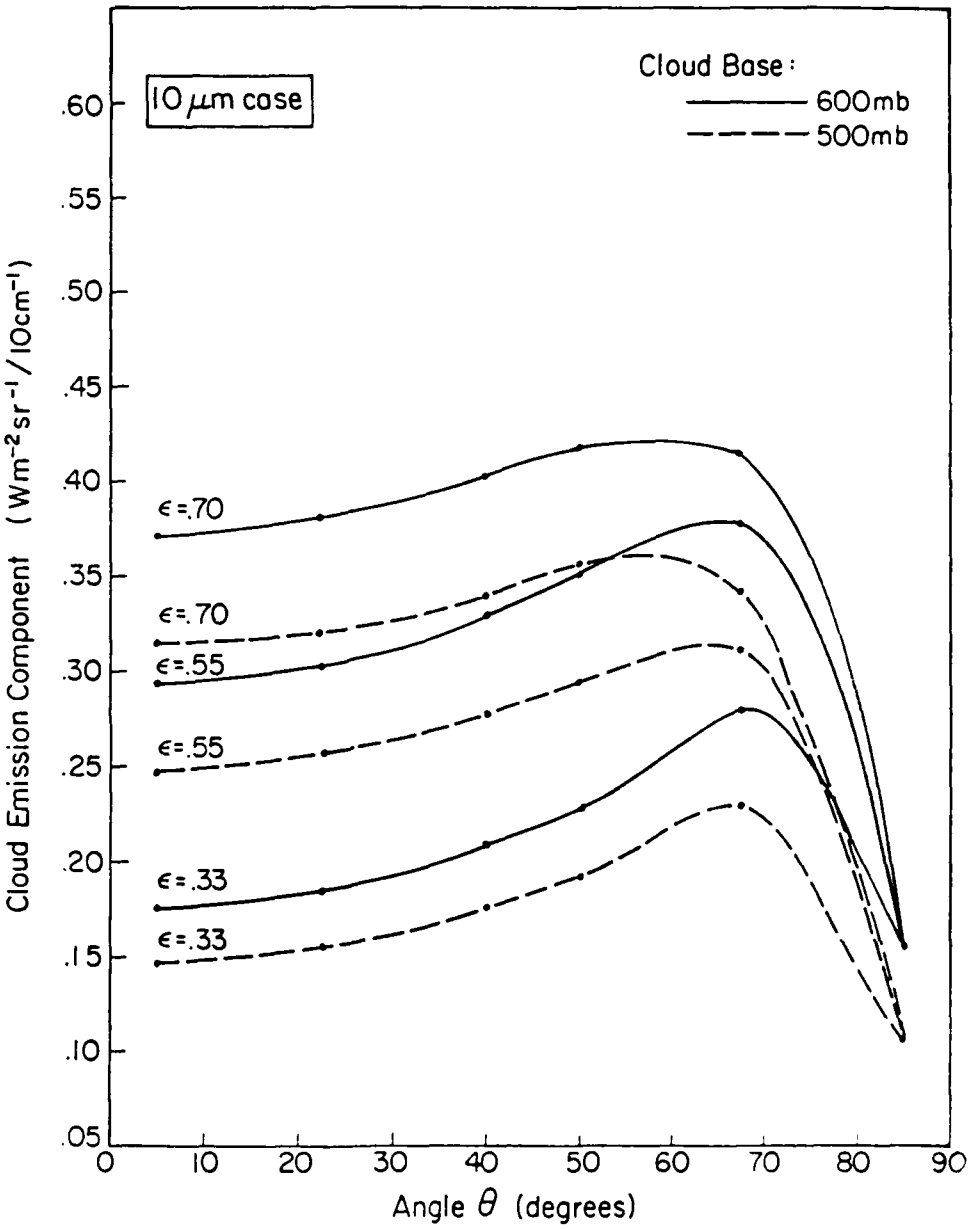

Fig. 6b. Cloud emission component as a function of zenith angle for the 500mb and 600mb cloud cases (10μm).

of .55 and the 500mb case with an emissivity of .70 both show 0° radiances of near .47$Wm^{-2}sr^{-1}/10cm^{-1}$. However, their respective radiances calculated near 65° are .615 and .575$Wm^{-2}sr^{-1}/10cm^{-1}$. The spread between the curves appears to decrease on either side of 65° and converge to near zero at 0° and 90°. Figure 6b shows the corresponding cloud emitted radiation curves as a function of zenith angle.

Figures 7a and 7b show comparison diagrams of the 500mb and 600mb cases computed at 11μm instead of 10μm. Since there is not a good example of a close match-up of radiances at 0° in figure 7a, it is difficult to quantify the radiance spread near 65°, as was done with the 10μm case. But the overall pattern of curves is similar. Each curve appears to be unique, and curves for clouds with different emissivities and heights cross at large angles. The existence of these characteristics is important for correlating a unique radiance curve with a unique cloud case. Figure 7b is the corresponding 11μm cloud emitted radiation diagram, but this time figure 7c has been included to focus in on the 40° to 90° region. This figure shows more precisely where cloud emission peaks occur. Instead of the peaks all falling at 67.50°, for instance, figure 7c confirms that the largest peaking angle is associated with the cloud at the lowest height and with the lowest emissivity, i.e. the 600mb cloud with an emissivity of .33 in this case. Unfortunately, because RADLON only calculates radiances at six quadrature angles at a time, pinpointing exact peak angles is not usually desirable, and is really not necessary.

If figures 6a and 7a are overlayed, significant differences in curve slopes appear. The 11μm curves have a larger spread of 0° radiances for both the 500mb and 600mb cases, and the curves change slope much more

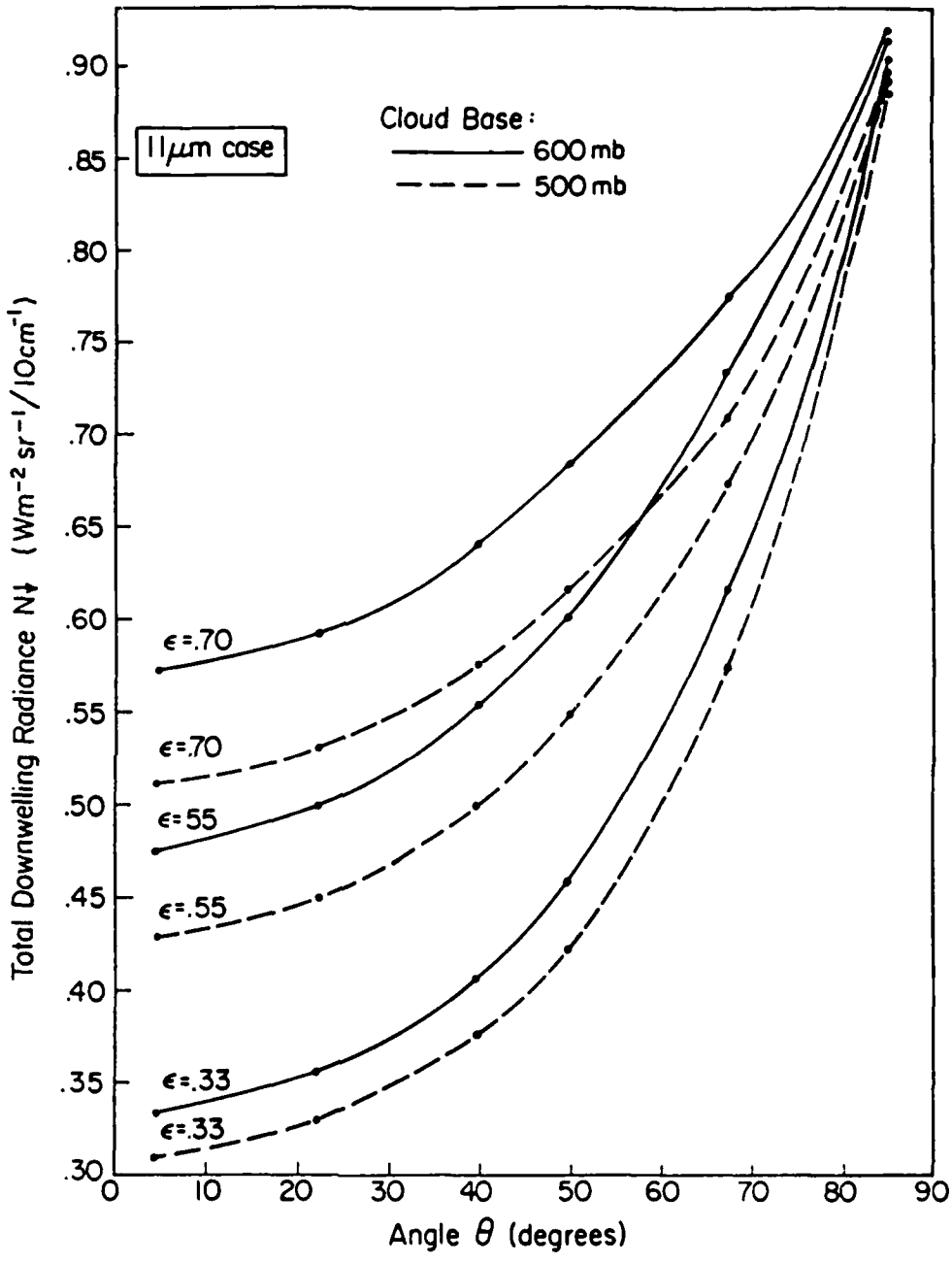

Fig. 7a. Total downwelling radiance curves as a function of zenith angle for the 500mb and 600mb cloud cases (11μm).

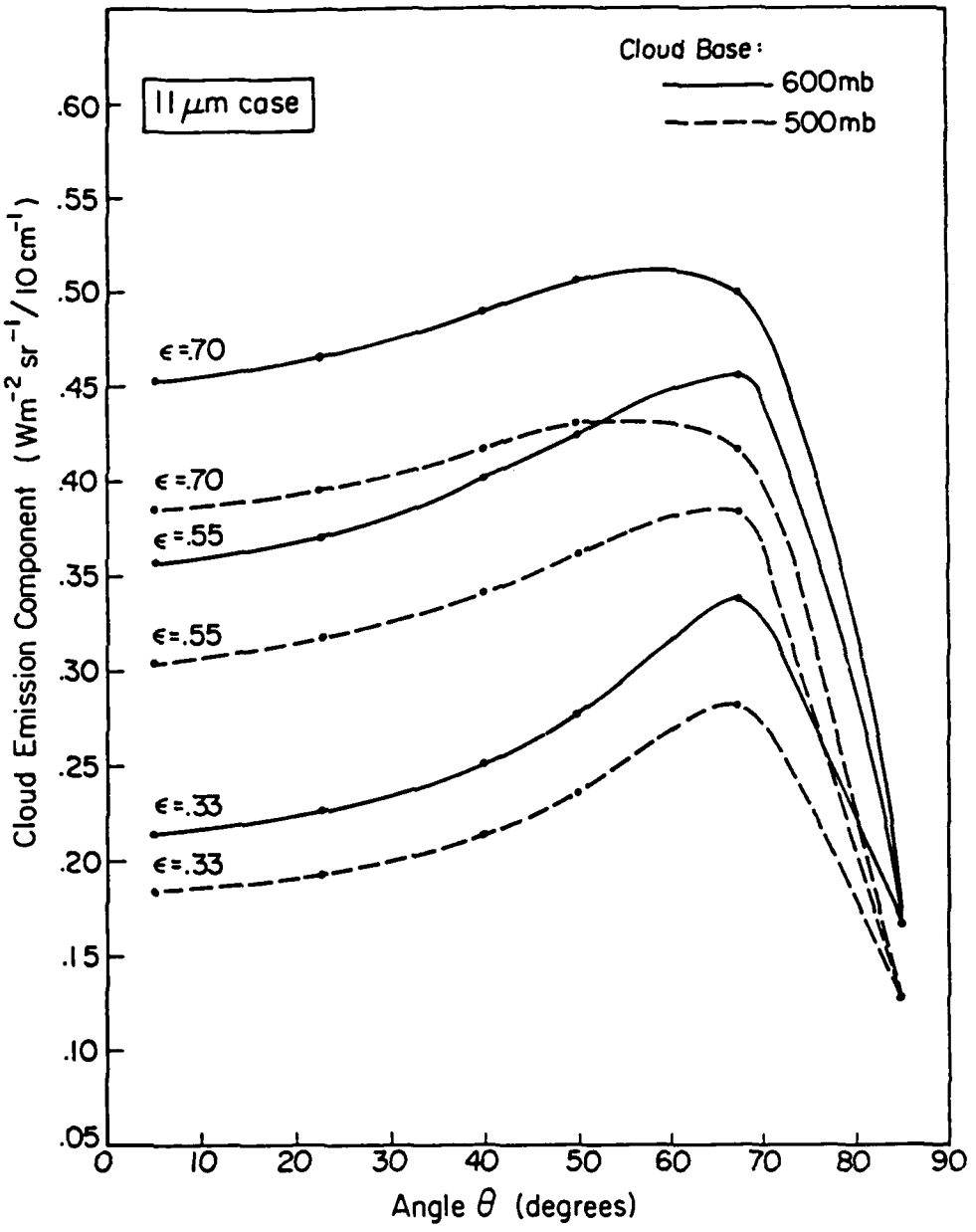

Fig. 7b. Cloud emission component as a function of zenith angle for the 500mb and 600mb cloud cases (11μm).

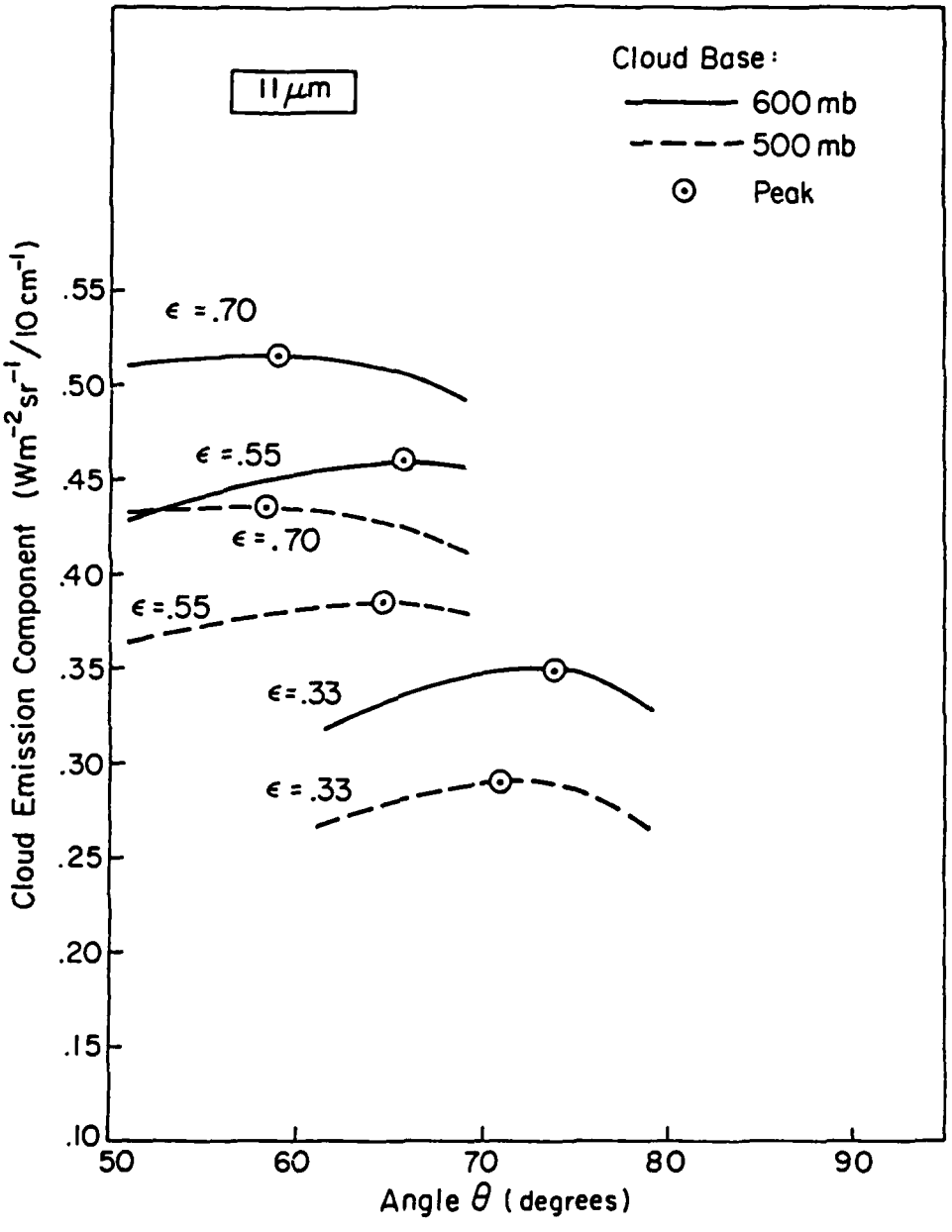

Fig. 7c. Cloud emission component maxima between 40° and 90° for the 500mb and 600mb cloud cases (11μm).

rapidly through 90° than did the 10μm curves. By overlaying figures 6b and 7b, the cloud emitted radiance curves, only minor differences can be seen. Their radiance values differ somewhat, but the patterns are nearly identical over 90°. Since some similarity appears in these cloud emission curves, the reason behind the difference in total radiance curves in figures 6a and 6b must be explained by something else. The explanation is likely due to the effects of ozone emittance above the cloud and incident on the cloud top at 10μm but not at 11μm. By taking ozone effects into account at 10μm, small angle radiation originating at the base of a low emissivity cloud resembles radiation associated with a higher emissivity. This effect tends to flatten and narrow the ground radiance curves at 10μm. At 11μm, however, the radiation incident on the top of the cloud is due only to water vapor and is relatively small. Therefore, in the following quantitative analyses for determining whether or not cloud base height and emissivity can be derived from angular radiances, it was important that both the 10μm and 11μm situations be tested and compared.

B. Solution for Cloud Height and Emissivity

As mentioned before, the radiance curves represented in Figure 4 are only a few examples of an infinite number of possibilities. Any observed radiance, by itself, could lie on an infinite number of curves. However, if radiances at more than one angle are observed for the same cloud layer, these radiances should form a curve that is unique for only one cloud layer. Knowing which curve matches which cloud is where some difficulties may lie. The purpose of this part of the investigation was to see if this type of match could be accomplished, with errors taken in

consideration, and if the choice of wavelength made a difference. Although conclusions were based on analyses between 500mb and 600mb, these conclusions provide some insight on whether or not this type of procedure has any merit at all.

1. Principles of Solution

It was previously determined that for radiance curves whose 0° radiances were nearly equal, the curves showed the greatest differences between 40° and 70° because of the angular effects of cloud emitted radiation that reaches the ground. Therefore, instead of having to make extensive radiance observations over many angles, comparisons of 0° radiances and 40°-70° radiances alone should correlate to one cloud case with a particular base height and emissivity. It is difficult to know which large angle radiances would be most useful, because it will differ for every case. However, since model radiance calculations from 0° to 90° were limited to six specific quadrature angles, the choice for the two angles was 5.07° for the small angle and 67.50° for the large angle. Only cloud levels between 600mb and 500mb were used, so the 67.50° angular radiances were ultimately chosen over the 50.07° radiances. On an average, cloud emission peaks in Figure 7b tended more towards 67.50° than 50.07°, except for the .70 emissivity cloud cases, making 67.50° a better choice.

2. Construction of Radiance Tables

Before an unknown cloud layer can be determined from observed radiances at 5.07° and 67.50°, tables must be constructed that contain radiances at those two angles which are believed to match all cloud

possiblities, such as data from figure 6a. For example, a cloud with a base at 600mb and an emissivity of .70, according to figure 6a, would give radiance measurements of approximately .525 and .645$Wm^{-2}sr^{-1}/10cm^{-1}$ at 5.07° and 67.50°, respectively. However, it is very important to keep in mind that these radiances were computed from a known temperature and moisture profile(figure 3). Ideally, if any clear sky atmospheric temperature and gas profile is known, similar model calculations can be made and tabulated for downwelling radiances at 5.07° and 67.50° for any cloud case. Unfortunately, the computer requirements would be quite extensive. Therefore, in order to simplify this investigation, tables of 5.07° and 67.50° radiances were constructed only for cloud cases between 500mb and 600mb.

The enormous radiance tables which could be generated for all cloud base heights and emissivities, even when only considering a region between 500mb and 600mb, were represented by two 5x5 tables--one for 5.07° and one for 67.50°. Small tables like these can actually represent an initial first guess at possible heights and emissivities of an unknown cloud layer. Separate tables were constructed for both 10μm and 11μm. These 5x5 tables included model radiance calculations for clouds at 570 mb, 575 mb, 580 mb, 585 mb, and 590 mb with corresponding emissivities of .40, .41, .42, .43, and .44. The 5mb and .01 intervals were arbitrary, but remain within the realistic limitations of sounding data and emissivity measurements. Tables 2a and 2b show the constructed 5.07° and 67.50° radiance tables for the 10μm and 11μm model calculations using the atmospheric profile of figure 3. These tables represent a small number of possible cloud cases, but if a cloud's height and emissivity can be determined to within 5mb and .01,

TABLE 2a

10μm Model Generated True Radiances($Wm^{-2}sr^{-1}/10cm^{-1}$)

Radiance Angle = 5.07°

Base Pressure(mb)	Spectral Emissivity .40	.41	.42	.43	.44
590.0	.4234	.4267	.4300	.4333	.4365
585.0	.4223	.4256	.4288	.4321	.4353
580.0	.4208	.4240	.4272	.4304	.4336
575.0	.4189	.4220	.4252	.4283	.4315
570.0	.4170	.4201	.4232	.4263	.4294

Radiance Angle = 67.50°

Base Pressure(mb)	Spectral Emissivity .40	.41	.42	.43	.44
590.0	.5906	.5933	.5959	.5985	.6010
585.0	.5889	.5915	.5941	.5966	.5991
580.0	.5865	.5891	.5917	.5942	.5966
575.0	.5836	.5861	.5886	.5911	.5934
570.0	.5807	.5832	.5856	.5880	.5903

TABLE 2b

11μm Model Generated True Radiances($Wm^{-2}sr^{-1}/10cm^{-1}$)

Radiance Angle = 5.07°

Base Pressure(mb)	Spectral Emissivity .40	.41	.42	.43	.44
590.0	.3757	.3820	.3883	.3946	.4010
585.0	.3744	.3807	.3870	.3933	.3996
580.0	.3727	.3789	.3851	.3914	.3976
575.0	.3705	.3767	.3829	.3890	.3952
570.0	.3684	.3745	.3806	.3867	.3928

Radiance Angle = 67.50°

Base Pressure(mb)	Spectral Emissivity .40	.41	.42	.43	.44
590.0	.6591	.6648	.6703	.6757	.6809
585.0	.6571	.6628	.6683	.6736	.6788
580.0	.6545	.6601	.6656	.6709	.6760
575.0	.6512	.6568	.6622	.6674	.6725
570.0	.6480	.6535	.6588	.6640	.6691

respectively, from these tables then they can most certainly be determined from larger tables. The radiance values shown in figures 8a and 8b will be referred to as "true" radiance values. Under ideal conditions, with no errors in radiances considered, only one set of true radiance observations at 5.07° and 67.50° would match any of the cloud cases represented. For example, at 10μm, a cloud with a base at 580mb and emissivity of .42 would only be identified if radiance observations at 5.07° and 67.50° were .4272 and .5917$Wm^2sr^{-1}/10cm^{-1}$, respectively. The next section will determine how much error can be associated with the observed 5.07° and 67.50° radiances and still result in the correct identification of a cloud.

3. Definition and Incorporation of Errors

An important point which must be considered in the construction of true radiance tables is that some error is likely to occur. A clear-sky temperature and moisture profile must be assumed from either climatological or radiosonde data. If the data is inaccurate, then the true radiance tables will also be inaccurate. For example, figure 8 shows one of many possible comparisons for how precipitable water beneath a cloud may change radiance measurements at the ground. Moisture was added independently to the 975-900mb, 850-750mb, and 750-600mb atmospheric layers for cloud cases based at 600mb and 500mb. Each time, the addition of moisture raised the precipitable water amount from 1.4cm to approximately 2.4cm and from 1.5cm to 2.4cm for the 600mb and 500mb cases, respectively. This diagram shows that additional moisture at any level still results in unique radiance curves, but if the existence of the moisture is unknown, i.e. the assumed moisture

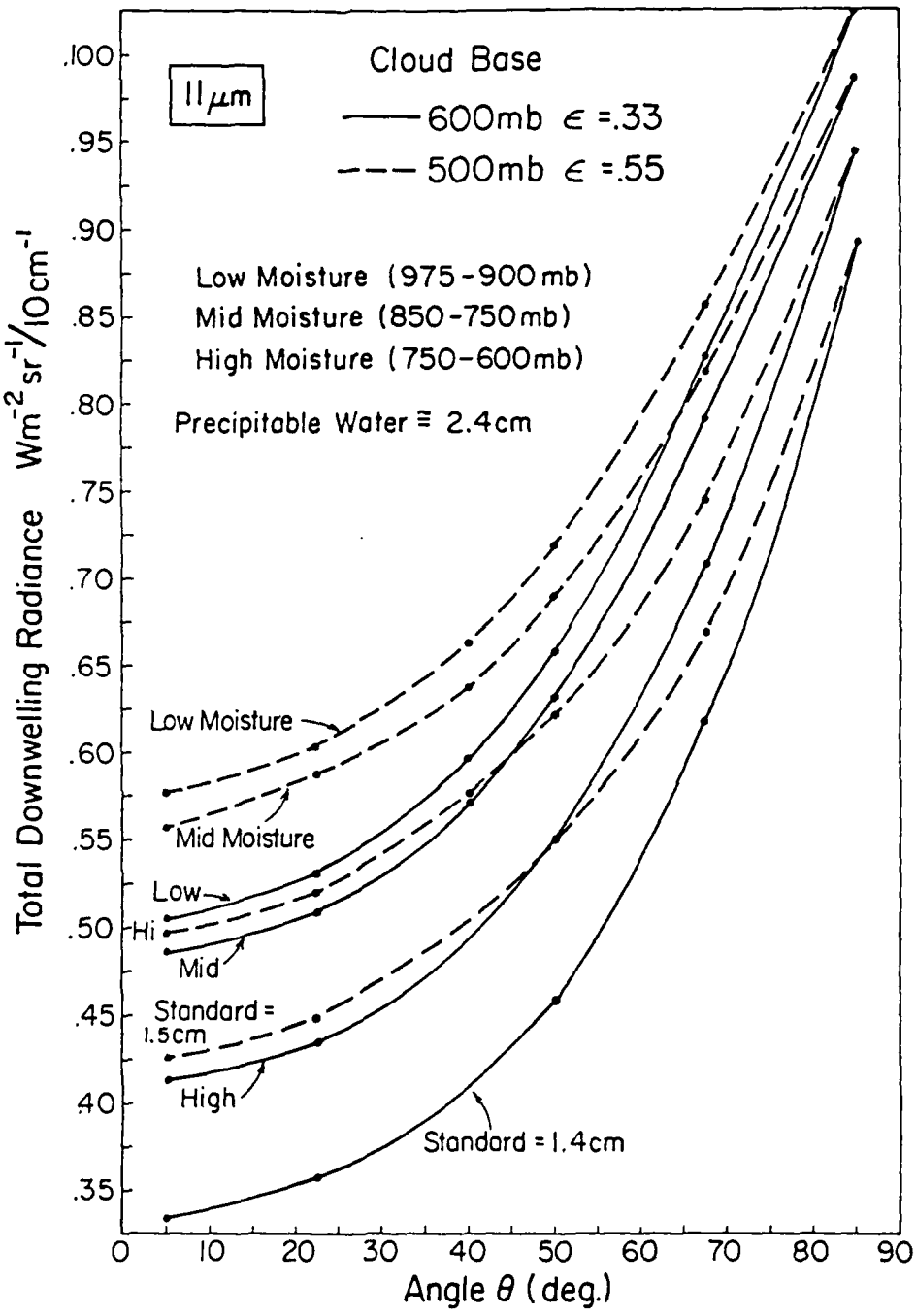

Fig. 8. Example comparison of total downwelling radiance curves for variations in the precipitable water for three levels beneath a cloud base.

profile is incorrect, predicted radiance curves could be in error by greater than 50%. The worst case situations occur when a lot of unknown moisture exists at low levels. For instance, the low level moisture radiance at 5.07° is 66% of the 0° radiance from the standard curve for the 600mb case. This type of error is extreme, but it should be considered for realtime radiance observations. Since this research does not involve realtime data, this type of error has been assumed negligible for simplicity. Therefore, the true radiances of tables 2a and 2b have been assumed error-free.

A certain amount of error is also usually assumed with any independent radiance observation. Oftentimes, especially in the case of meteorological instruments, thi error is quoted as a relative error. A certain percentage of the true value is allowed on either side of that true value. Relative error eliminates the problem of units but may allow slightly more error in larger measurements of the same property. Radiance observations match the true radiances in tables 2a and 2b if they fall within the specified error range on either side of the true radiance. Different amounts of error were tested to determine when the 5.07° and 67.50° observed radiances resulted in an incorrect cloud height and emissivity.

In tables 2a and 2b, radiances don't vary much for pressure changes of 5mb or for emissivity changes of .01. Therefore, in order to maintain correct matches between 5.07° and 67.50° radiances, errors were expected to be quite small. A large error in one of the radiance observations could cause more than one match or no match to occur. Larger errors would be possible if the pressure level and emissivity increments used to construct the radiance tables were increased, say

50mb versus 5mb, but the height and emissivity of a cloud could not be narrowed down as well. Therefore, even though this study only investigated determining cloud base pressure to within ±5mb and an emissivity to within ±.01, error tolerance for radiance observations depend on the desired degree of accuracy for cloud height and emissivity.

4. Generation of Test Cases and Results

Combinations of realistically possible 5.07° and 67.50° observed radiances, with randomly generated errors, were tested at 10μm and 11μm to see if they could be matched in Tables 2a or 2b(depending on the wavelength) to determine a particular cloud height and emissivity. All tests were done using the 580mb cloud height with an emissivity of .42 as the correct cloud condition. The amount of error associated with each angular radiance determined whether or not this correct cloud case could be identified. The purpose of the testing was to determine the largest amount of error that could be assumed for both radiance observations and still result in the correct cloud height and emissivity. This error was expressed in terms of a percentage of the true radiance.

A random number generator(MINITAB) was used to create radiance pairs for the 5.07° and 67.50° angles. The radiance pairs were created by adjusting each independent radiance with a randomly generated percentage error. Errors associated with each independent radiance observation were categorized as being one of two types; either normally distributed or a bias in one particular direction. Random radiance pairs that had normally distributed errors were calculated using:

$$N(random) = N(true) \times (1. + random\ percent\ error)$$

where N represents radiance, and the percent error was randomly generated from a normal distribution with a mean of zero and a standard deviation of a specified percentage. This percentage was the error tolerance being tested, error tolerance referring to the amount of error allowed on either side of a true radiance that can still result in a match. For example, if a 1% error tolerance was being tested, a random radiance observation would match N(true) if it fell within N(true)±(.01xN(true)). A mean of zero and a standard deviation of .01 would be input into the random number generator so as to create normally distributed random errors. MINITAB does not use the same initial random numbers, scaled according to the standard deviation, each time a new set of random numbers is generated. Therefore, multiple sets of repeat tests had to be done to make up for the inability to compare error tolerances based on the same data.

Once random errors were generated and random radiance pairs at 5.07° and 67.50° were created, each pair was input into a program called SEARCH that attempted to match both radiances to the 580mb height and .42 emissivity in tables 2a and 2b, despite the errors that existed. A flowchart of the program SEARCH is given in figure 9. For each 5.07° radiance match, and there could easily be more than one, 67.50° radiances were also sought until the corresponding base pressures converged. The emissivity was then retrieved from the appropriate column. If pressures did not converge, then the closest match was noted.

For normally distributed random errors, ten random radiance pairs were tested for several error tolerances at both 10μm and 11μm. Tested

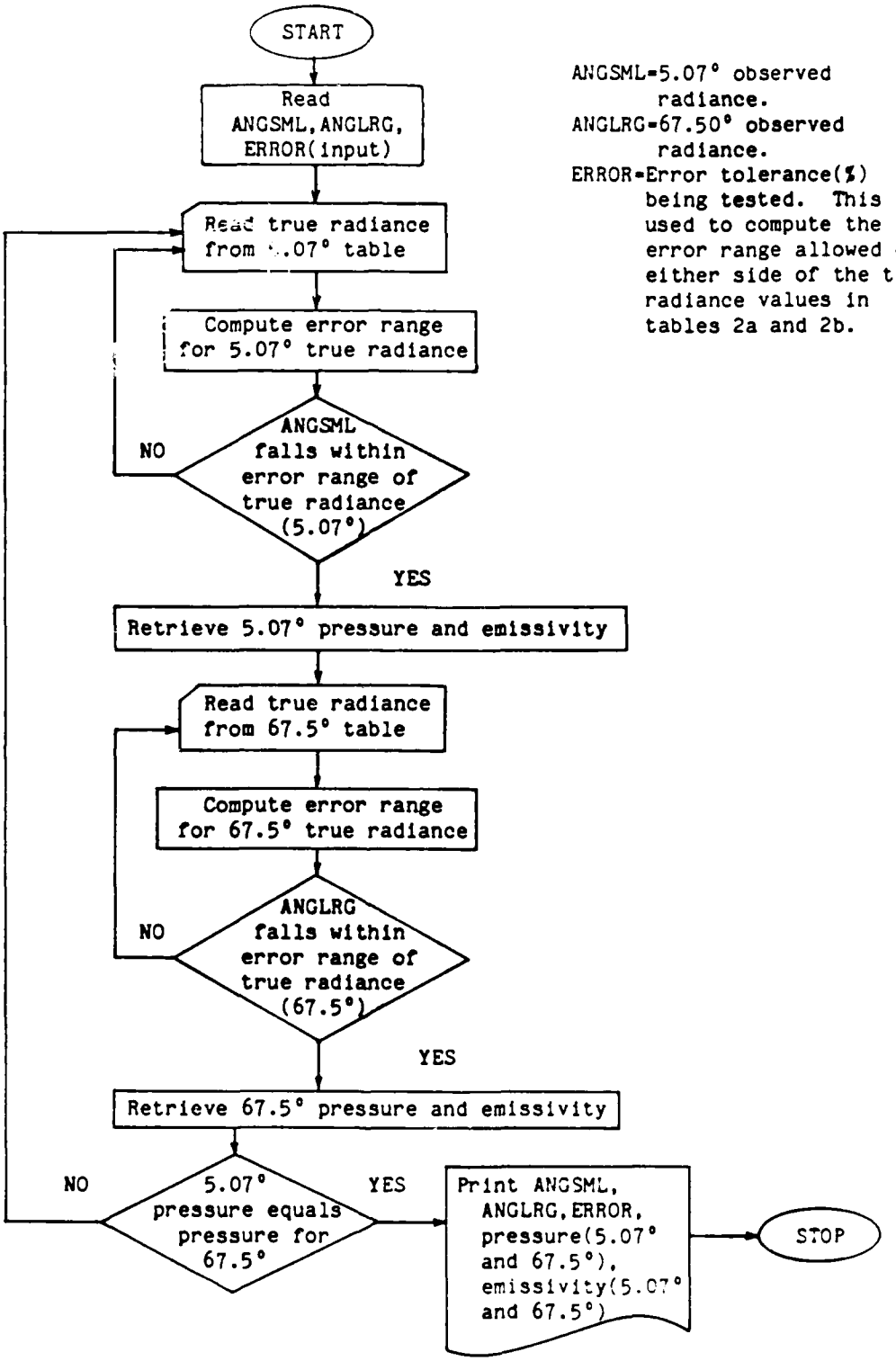

Fig. 9. Flowchart for program SEARCH. This program matches 5.07° observed radiances and 67.50° observed radiances with "true" angular radiances to obtain an estimate of an unknown cloud height and emissivity.

error tolerances began at 1% and decreased by .05% until 7 out of 10 searches through the appropriate table resulted in the correct identification of a cloud at 580mb with an emissivity of .42. This 70% error-free criterion was chosen so that the chance of success closely followed a normal distribution. Once the 70% criterion was reached, four more tests were repeated for this same standard deviation to make sure that the one successful test wasn't just a lucky production of good random errors. This was the one disadvantage of using a random number generator that didn't produce identical errors, scaled according to the standard deviation, each time new numbers were computed. At 10μm, an error tolerance of .1% met the 70% criterion. At 11μm, an error tolerance of .25% met the criterion. Table 3a shows two representative examples of 10μm error test cases, including the first .1% case and the results of its four additional tests. The table shows ten separate trials of ten random radiance pairs, N '(5.07°) and N '(67.50°), with the resultant errors in cloud height and emissivity determination, $P_{true}-P'$ and $\varepsilon_{true}-\varepsilon'$. The .5% example shows that clouds can be incorrectly identified by at least 10mb if the error tolerance is too high. Although all of the five trials for .1% didn't result in a 70% error-free rate, the average of the five did. Table 3b shows two examples of the 11μm tests, including the five test results at .25%.

Bias error analysis was simpler than the normal distribution analysis, but based on the same search and match principles. The bias errors were preset as specific plus or minus percentages, such as positive .5% or negative 1%. Since all random errors were assumed to fall within this percentage range, only the extreme cases were tested. If an error was equal to the maximum bias but could still result in

TABLE 3a

10μm Sample of Normally Distributed Random Errors

N(true,5.07°)= .4272$Wm^{-2}sr^{-1}/10cm^{-1}$
N(true,67.5°)= .5917$Wm^{-2}sr^{-1}/10cm^{-1}$
Pressure(true)= 580mb
Spectral Emissivity(true)= .42

Error Tolerance (standard deviation) = .5%

Trial	Random Error (small/large)	N' (5.07°)	N' (67.5°)	P' (mb)	ε'	P(true)-P' (mb)	ε(true)-ε'
1	-.0027/.0061	.4260	.5953	590	.41	+10	-.01
2	.0031/.0050	.4285	.5946	590	.41	+10	-.01
3	.0064/.0045	.4299	.5943	590	.42/.41	+10	-.005
4	.0020/.0040	.4280	.5940	590	.41	+10	-.01
5	-.0012/-.0035	.4266	.5896	590	.41/.40	+10	-.015
6	.0020/-.0063	.4280	.5879	590	.41/.40	+10	-.015
7	-.0065/-.0051	.4244	.5886	590	.40	+10	-.020
8	.0012/.0026	.4277	.5932	590	.41/.40	+10	-.015
9	.0026/-.0005	.4283	.5914	590	.41/.40	+10	-.015
10	.0007/.0006	.4274	.5920	590	.41/.40	+10	-.015

TABLE 3a(cont)

Error Tolerance (standard deviation) = .1%

Trial	Random Error (small/large)	N' (5.07°)	N' (67.5°)	P' (mb)	ε'	P(true)-P' (mb)	ε(true)-ε'
1	-.0008/-.0003	.4268	.5915	580	.42	0	0
2	.0001/-.0002	.4272	.5915	580	.42	0	0
3	.0022/-.0009	.4281	.5911	575	.43	-5	+.01
4	-.0001/.0006	.4271	.5920	580	.42	0	0
5	-.0001/.0007	.4271	.5921	580	.42	0	0
6	.0006/-.0009	.4274	.5911	580/575	.42/.43	-2.5	+.005
7	.0005/.0004	.4274	.5919	580	.42	0	0
8	-.0015/-.0015	.4265	.5908	590	.41/.40	+10	-.015
9	.0010/-.0004	.4276	.5914	580	.42	0	0
10	-.0003/.0002	.4270	.5918	580	.42	0	0

Repeat Tests of .1%:

Trial	Success Rate
1	60%
2	60%
3	70%
4	80%

TABLE 3b

11 μm Sample of Normally Distributed Random Errors

N(true,5.07°)= .3851 $Wm^{-2}sr^{-1}/10cm^{-1}$
N(true,67.5°)= .6659 $Wm^{-2}sr^{-1}/10cm^{-1}$
Pressure(true)= 580mb
Spectral Emissivity(true)= .42

Error Tolerance (standard deviation) = .5%

Trial	Random Error (small/large)	N' (5.07°)	N' (67.5°)	P' (mb)	ε'	P(true)-P' (mb)	ε(true)-ε'
1	.0030/-.0038	.3862	.6633	585	.42/.41	+5	-.005
2	-.0013/.0014	.3845	.6683	580	.42	0	0
3	-.0052/.0077	.3830	.6710	590	.41/.42	+10	-.005
4	.0003/.0044	.3852	.6688	585	.42	+5	0
5	-.0020/-.0085	.3843	.6715	580	.42/.43	0	+.005
6	-.0060/.0065	.3827	.6702	590	.41/.42	+10	-.005
7	.0029/.0081	.3862	.6712	585	.42	+5	0
8	.0013/.0058	.3856	.6697	585	.42	+5	0
9	-.0084/-.0147	.3818	.6561	590	.41/.40	+10	-.015
10	.0117/.0004	.3896	.6661	590	.42/.41	+10	-.005

TABLE 3b(cont)

Error Tolerance (standard deviation) = .25%

Trial	Random Error (small/large)	N' (5.07°)	N' (67.5°)	P' (mb)	ε'	P(true)-P' (mb)	ε(true)-ε'
1	.0051/.0030	.3870	.6678	585	.42	+5	0
2	-.0010/.0005	.3847	.6662	580	.42	0	0
3	-.0003/.0031	.3849	.6679	580/575	.42/.43	-2.5	+.005
4	.0012/-.0021	.3855	.6645	580	.42	0	0
5	-.0010/.0015	.3847	.6668	580	.42	0	0
6	-.0009/.0021	.3847	.6672	580	.42	0	0
7	-.0002/.0030	.3850	.6678	580/575	.42/.43	-2.5	+.005
8	-.0020/-.0014	.3843	.6649	580	.42	0	0
9	.0009/.0009	.3854	.6664	580	.42	0	0
10	-.0008/-.0008	.3850	.6653	580	.42	0	0

Repeat Tests of .25%:

Trial	Success Rate
1	70%
2	90%
3	80%
4	70%

correct cloud identification, smaller errors were also assumed to work. In other words, if a bias error of +.5% was being tested, the 5.07° and 67.50° true radiances were offset by +.5% and tested.

Bias error test cases were based on the above results of the normal distribution cases. It was assumed that error tolerances smaller than .1% and .25% for 10μm and 11μm, respectively, would also result in a correct cloud identification, making these tests unnecessary. As mentioned before, only extreme cases were considered, i.e. tests were done only for radiance observations that were on the edge of the prescribed error tolerance. Tables 4a and 4b show the 10μm and 11μm tests that were performed up to a bias of ±1%.

C. Discussion of Results

The 10μm and 11μm error test cases described above bring out two important results. First of all, wavelength tests for normally distributed and biased errors showed that a very small error tolerance must be assumed in order to correctly identify a cloud height and emissivity within 5mb and .01, respectively. Considering the errors that may be involved in initially determining true radiance tables and those involved with obtaining radiance observations at 5.07° and 67.50°, .1% and .25% error tolerances seem unrealistically small. These error tolerances, of course, are dependent on how precise the cloud height and emissivity determinations must be. For instance, they would probably be larger if the cloud height needed to be to the closest 50mb instead of 5mb.

The second important result was that the 11μm tests allowed more error than the 10μm tests. These particular tests showed twice as much

TABLE 4a

10μm Sample of Bias Errors

N(true,5.07°)= .4272$Wm^{-2}sr^{-1}/10cm^{-1}$
N(true,67.5°)= .5917$Wm^{-2}sr^{-1}/10cm^{-1}$
Pressure(true)= 580mb
Spectral Emissivity(true)= .42

Error Threshold (%)	N' (5.07°)	N' (67.5°)	P' (mb)	ε'	P(true)-P' (mb)	ε(true)-ε'
+.10	.4276	.5922	580	.42	0	0
-.10	.4267	.5911	580	.42	0	0
+.12	.4277	.5924	580	.42	0	0
-.12	.4266	.5909	590	.41/.40	+10	0
+.15	.4278	.5925	580	.42	0	0
-.15	.4265	.5908	590	.41/.40	+10	-.015
+.20	.4280	.5928	580	.42	0	0
-.20	.4263	.5905	590	.41/.40	+10	-.015
+.30	.4284	.5934	585	.42	+5	0
-.30	.4259	.5899	590	.41/.40	+10	-.015
+.50	.4293	.5946	590	.42/.41	+10	-.005
-.50	.4250	.5887	590	.40	+10	-.020
+1.00	.4314	.5976	590	.42/.41	+10	-.005
-1.00	.4229	.5857	590	.40	+10	-.020

TABLE 4b

11μm Sample of Bias Errors

N(true,5.07°)= .3851$Wm^{-2}sr^{-1}/10cm^{-1}$
N(true,67.5°)= .6659$Wm^{-2}sr^{-1}/10cm^{-1}$
Pressure(true)= 580mb
Spectral Emissivity(true)= .42

Error Threshold (%)	N' (5.07°)	N' (67.5°)	P' (mb)	ε'	P(true)-P' (mb)	ε(true)-ε'
+.25	.3860	.6675	580	.42	0	0
-.25	.3841	.6642	580	.42	0	0
+.30	.3862	.6678	585	.42	+5	0
-.30	.3839	.6639	575	.42	-5	0
+.40	.3866	.6685	585	.42	+5	0
-.40	.3835	.6632	590	.41	+10	-.01
+.50	.3870	.6692	590	.42	+10	0
-.50	.3831	.6625	590	.41	+10	-.01
+1.00	.3889	.6725	590	.42	+10	0
-1.00	.3812	.6592	590	.41/.40	+10	-.015

error could be tolerated at 11μm. This was somewhat expected. It is evident from tables 2a and 2b that larger changes occur in 11μm radiances than 10μm radiances for a constant change in pressure or emissivity. Therefore, searches through an 11μm table would be more likely to single out a unique match than would searches through a 10μm table. Regardless of the numerical error values that were computed for 10μm and 11μm, angular radiance observations at 11μm appear to be better indicators of a cloud's height and emissivity than at 10μm. These, however, are only two representative atmospheric window wavelengths. Conclusions made from this investigation may or may not be applicable to other wavelengths.

D. Broadband Emissivity

The previous test cases indicate that a cloud's base height and spectral emissivity can be estimated, with a limited amount of error, from known 5.07° and 67.50° radiances. Once the height and emissivity is obtained, a broadband emissivity can also be inferred. Figure 10 (Yamamoto,1969) shows spectral emissivities for wavelengths between 5-50μm as a function of wavenumber and cloud thickness. In this case, cloud thickness (X_1) is defined as the total optical thickness divided by the extinction coefficient of the cloud, which is a function of the water content of the cloud. The curves for X_1 equal to 2m to infinity provide representative examples of very thin to thick clouds. By computing a weighted average across the 2m, 10m, 50m, and infinity curves in figure 10, an average broadband emissivity can be calculated for 5-50μm for each case. This broadband emissivity is dependent on the temperature of the cloud. Equation 9 can be used to determine the

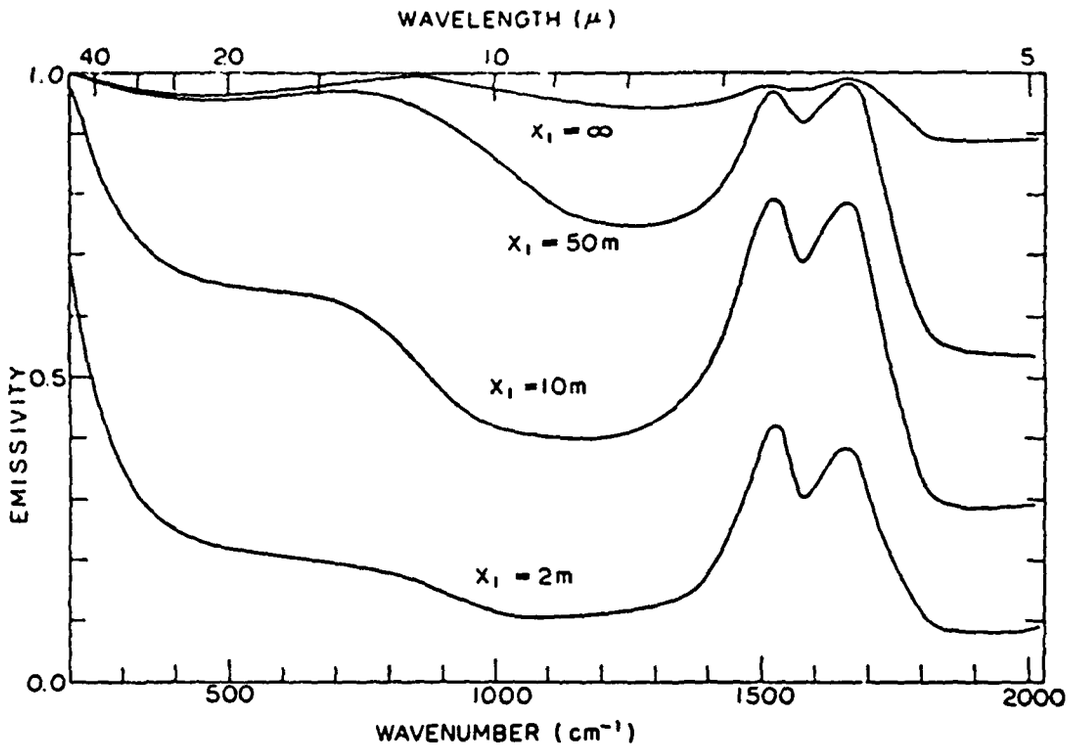

Fig. 10. Spectral emissivity of clouds of various thicknesses vs wavenumber or wavelength, reproduced from Yamamoto, 1969.

weighted, average emissivity for the four cloud cases at any temperature:

$$\bar{\varepsilon}(T,X_1) = \Sigma(\varepsilon_\nu)B(T,\nu) \;/\; \Sigma B(T,\nu) \qquad (9)$$

where $\bar{\varepsilon}(T,X_1)$ is the broadband emissivity, $B(T,\nu)$ is the temperature and wavenumber dependent Planck function, and ε_ν is the spectral emissivity taken from figure 10 (for every $100cm^{-1}$) for X_1 equal to 2m, 10m, 50m, and infinity.

As an example, broadband emissivities were calculated for a range of cloud temperatures from +16°C to -36°C; this covers the temperature range of the initial seven cloud cases described in section III.A.3. Figure 11 shows calculated broadband emissivities as a function of 10μm ($\nu = 1000cm^{-1}$) emissivities obtained from the four X_1 curves in figure 10. The two curves in figure 11 are for cloud temperatures of +16°C and -36°C only. All other temperature curves lie within these two curves. The maximum variation between the broadband emissivity curves for +16°C and -36°C is approximately .04.

The MINITAB statistical package that was used to generate random numbers was also used to fit the two curves in figure 11. A quadratic regression model of the form $Y = b_o + b_1x + b_2x^2$ was used to derive formulas for both curves. The two formulas for the +16° and -36° broadband emissivity curves are given by equation 10 and 11, respectively:

$$\bar{\varepsilon}(\varepsilon_\nu) = .0342 + 1.63(\varepsilon_\nu) - .690(\varepsilon_\nu)^2 \qquad (10)$$

$$\bar{\varepsilon}(\varepsilon_\nu) = .0466 + 1.75(\varepsilon_\nu) - .824(\varepsilon_\nu)^2 \qquad (11)$$

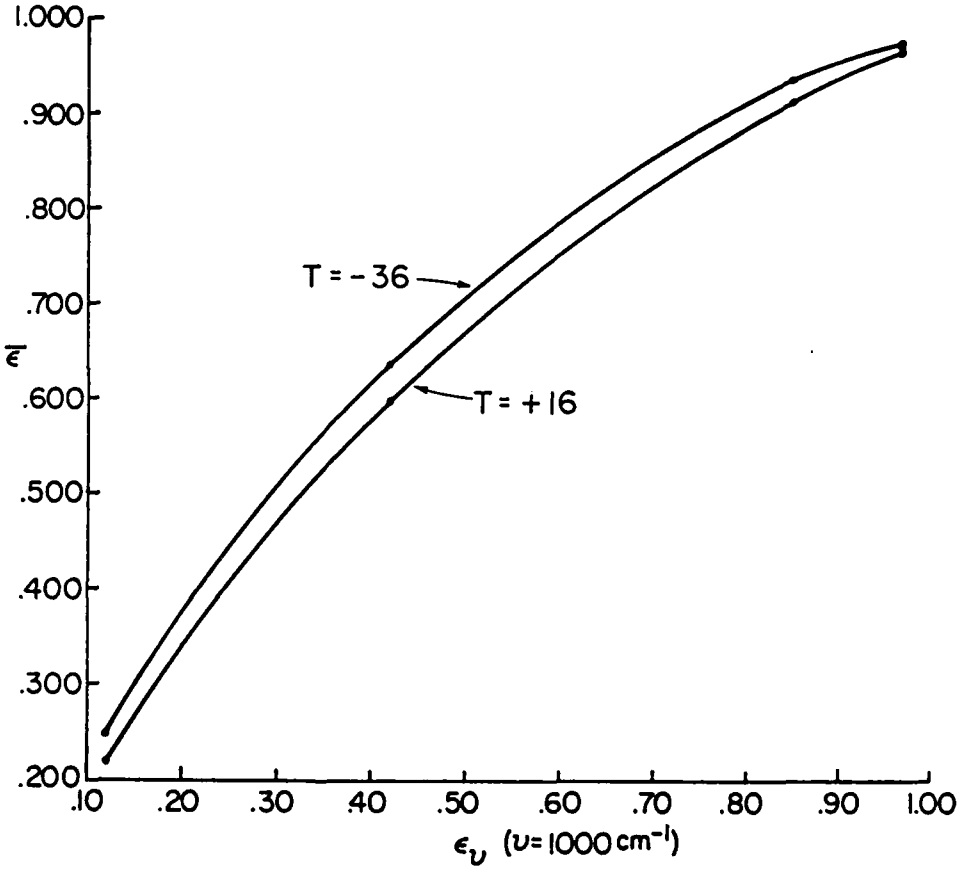

Fig. 11. Broadband emissivity as a function of 10μm spectral emissivity for -36°C and +16°C cloud base temperatures.

where ν=1000cm^{-1}. The average deviation from these mean equations was .0076 and .0034, respectively.

By using equations 10 and 11, a broadband emissivity can now be inferred from a known 10μm spectral emissivity and cloud temperature. The base temperature of a cloud can be estimated from its base height and an appropriate atmospheric temperature profile, such as was shown in figure 3. For a given 10μm spectral emissivity, $\bar{\varepsilon}(\varepsilon_\nu)$ from the +16° curve and $\bar{\varepsilon}(\varepsilon_\nu)$ from the -36° curve can be obtained. Once these broadband emissivities are known, linear interpolation can be performed for the broadband emissivity that corresponds to the temperature of the cloud. Similarly, this same procedure can be applied for other spectral emissivities, as long as equations 10 and 11 are adjusted for the wavelength being used.

E. Summary of Solution Procedures

Figure 12a has been provided to summarize the model demonstration used in the previous sections. This figure outlines the major steps needed to estimate the base height, spectral and broadband emissivities of an unknown homogeneous cloud layer from downwelling radiances at two zenith angles. Figure 12b is a consolidation of the major equations used in the demonstration. The concepts incorporated into both figures were based on the following assumptions:

1. A clear-sky temperature/moisture profile can be obtained.

2. The atmosphere can be divided into homogeneous, stratified layers.

3. The unknown cloud layer is isothermal, microphysically homogeneous, and has a constant thickness and height.

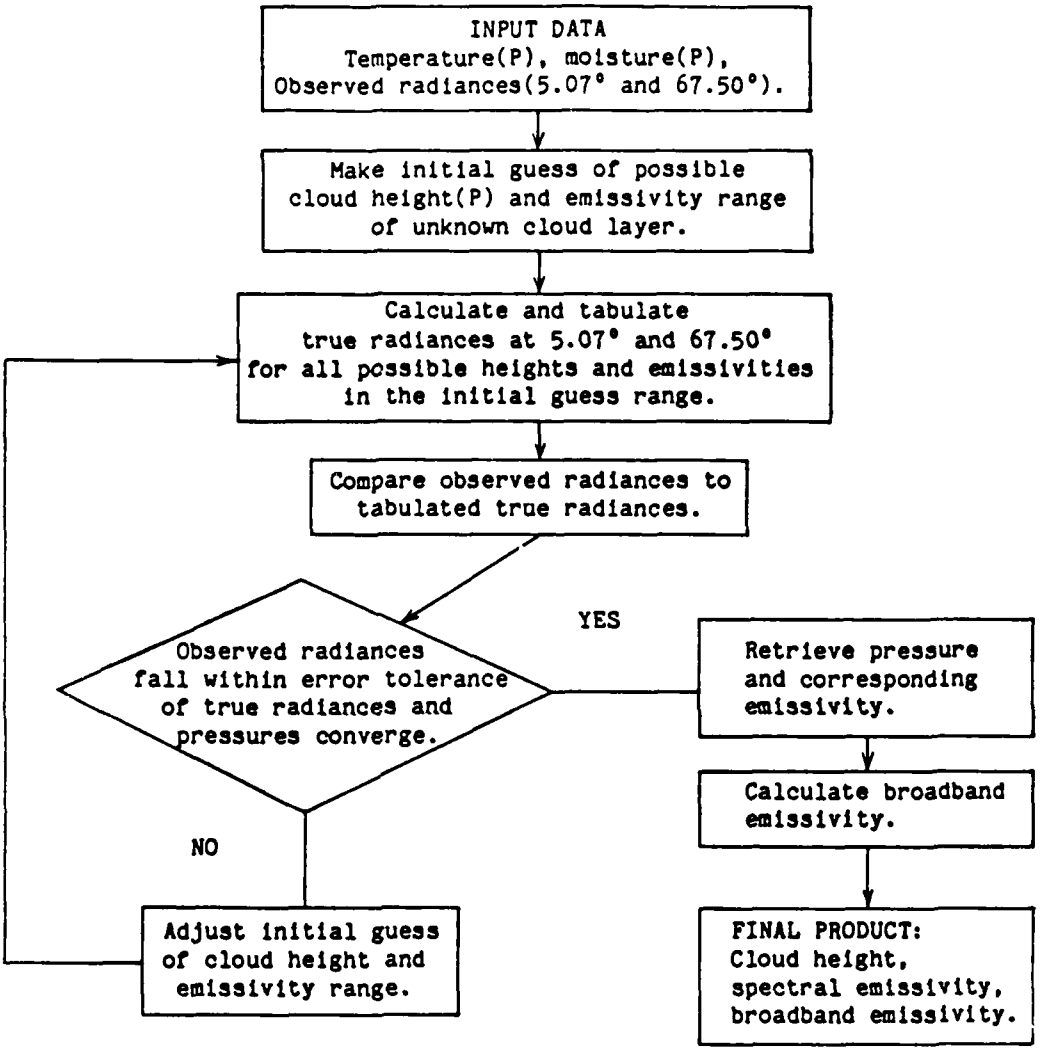

Fig. 12a. Summary of model demonstration used to determine the height and emissivity of an unknown cloud layer.

I. Calculation and tabulation of true radiances at 5.07° and 67.50°:

A. Radiative transfer equation for a homogeneous greybody cloud layer (reflectivity = 0).

$$N\downarrow(\nu,\tau,-\mu) = \int_{\tau_B}^{\tau_1} J(\nu,t)e^{(t-\tau_1)/\mu}\,dt/\mu +$$
$$\{(\varepsilon_\lambda)B(\nu,T_{cloud}) + [(1-\varepsilon_\nu)\int_{\tau_0}^{\tau_T} J(\nu,t')e^{(t'-\tau_T)/\mu}\,dt/\mu]\}e^{(\tau_B-\tau_1)/\mu}$$

where

$$\varepsilon_\theta = 1. - (1.-\varepsilon_o)^{\sec\theta}$$

$$B_\nu(T) = 2h\nu^3/c^2[\exp((h\nu/KT)-1)]$$

II. Observed radiance falls within error tolerance of the true radiance.

A. Normal random error:

N(true)-(random error x N(true)) ≤ N(observed) ≤ N(true)+(random error x N(true))

B. Bias error:

N(true) ≤ N(observed) ≤ N(true) + (bias error x N(true))

N(true) ≥ N(observed) ≥ N(true) - (bias error x N(true))

III. Broadband emissivity:

A. Weighted, average broadband emissivity as a function of spectral emissivity and Planck function.

$$\bar{\varepsilon}(T,X_1) = \Sigma(\varepsilon_\nu)B(T,\nu) \;/\; \Sigma B(T,\nu)$$

B. Polynomial regression formula for $\bar{\varepsilon}$ as a function of ε_ν. (Temperature = constant)

$$\bar{\varepsilon}(\varepsilon_\nu) = b_o + b_1(\varepsilon_\nu) + b_2(\varepsilon_\nu)^2$$

Fig. 12b. Summary of major equations used in model demonstration.

4. Reflectivity can be neglected for infrared calculations.

5. The spectral emissivity of a cloud is based on equation 7, and is only a function of the zenith angle and the 0° emissivity.

6. Radiance calculations cover a $10cm^{-1}$ wavenumber interval.

Although this demonstration was based on one specific cloud case study, the procedures and equations outlined in figures 12a and 12b should be applicable to other homogeneous cloud situations.

V. CONCLUSION

A technique has been devised which uses ground-based radiance observations to estimate the base height and spectral emissivity of a homogeneous cloud layer. From the spectral emissivity, a broadband emissivity can also be deduced. Errors were incorporated to simulate what could be observed using actual meteorological equipment, such as radiometers and radiosondes. Model calculations at 10μm and 11μm showed that homogeneous cloud layers produce unique sets of ground radiance values over a range of zenith angles from 0° to 90°. By examining downwelling ground radiances at a very small zenith angle and a second zenith angle between 40° and 80°, one can distinguish between low emissivity-low clouds and high emissivity-high clouds. This is possible because the cloud emissivity and the atmospheric transmissivity beneath a cloud are dependent on the viewing angle, thus affecting how much radiation reaches the ground; as a result, this relationship differs for every cloud height and emissivity.

A summary of the important points that arose from the analysis of angular downwelling radiances associated with clouds is as follows:

1. Downwelling radiance values from 0° to 90° appear to be unique for homogeneous grey body cloud layers. Any single value can be associated with an infinite number of possible cloud cases. However, no two cloud cases produced exactly the same ground radiances over all angles.

2. The change in cloud emissivity and the concurrent change in atmospheric transmissivity beneath a cloud as a function of angle appear to be primarily responsible for the existence of unique radiance curves. As the viewing angle increases from 0° to 90°, the emissivity of a cloud will eventually approach 1.0. At the same time, the transmissivity of the intervening atmosphere beneath the cloud will exponentially decrease. Before the atmosphere becomes nearly opaque to cloud emitted radiation, the cloud emission that reaches the ground will reach a maximum between 40° and 70°. The precise peaking angle differs for every cloud configuration, depending on height, wavelength, the temperature/moisture profile, and initial 0° emissivity. Although clouds may result in nearly equal ground radiances at small angles, the difference in cloud emission maxima cause radiance curves to separate at larger angles.

3. By constructing two ground radiance tables at two angles for all combinations of cloud heights and emissivities, radiance observations at near 0° and a larger angle can be used to estimate the unknown height and spectral emissivity of a cloud layer. The radiance tables are calculated from the known clear sky atmospheric temperature and gas profiles. In this study, radiances at 5.07° and 67.50° were sought in the tables until they were matched to the same cloud base height(in pressure). The 0° spectral emissivity that correlated to this height and the observed radiances was then retrieved. A broadband infrared emissivity can then be inferred from the spectral emissivity.

4. Estimations of cloud height and emissivity are more accurately determined using 11μm radiance observations rather than 10μm observations. An error tolerance of .1% was required at 10μm to

correctly determine the height and emissivity of a cloud to within 5mb and .01, respectively, 70% of the time. An error tolerance of .25% was required at 11μm. These were the only two wavelengths tested. Since only two wavelengths were compared, further examination of other atmospheric window wavelengths may prove beneficial.

5. Conclusions presented in this research are based on nearly ideal model calculations and must be tested using actual angular radiance data. For any radiance measurements, there are three major sources of error that could cause these measurements to identify the wrong cloud. The first source of error is related to obtaining an inaccurate clear-sky temperature/moisture profile from climatological or radiosonde data. This may be the most significant source of error, but was not specifically addressed in this research. A second likely source of error is due to instrumentation used for radiance measurements. This is not, however, an error that can be attributed to the procedure presented in this research for identifying a cloud, but should be considered when using actual radiance observations. The third source of error lies in the fact that nature rarely produces homogeneous cloud layers that extend horizontally far enough so that radiance measurements can be made over large angles.

6. There is still valuable research to be done that can stem from this initial investigation. First of all, cloud heights outside of the 500mb to 600mb range used in this research should be considered. Clouds near and above 300mb may be more difficult to distinguish because of their cold temperatures and a deeper intervening atmosphere beneath them. Secondly, future research could investigate temperature and moisture profiles from different climatological regimes. These regimes could

include tropical, polar, arid and oceanic regions, plus regions of highly variable topography. Complicated profiles, such as those with inversions or synoptic/mesoscale features, could also be examined. Thirdly, more sophisticated techniques should be explored for determining a cloud's base pressure and emissivity from downwelling angular radiances. Advanced computer algorithms could possibly avoid tedious searches through radiance tables based on specific pressure and emissivity intervals. Finally, theoretical studies should be compared with real radiance data. If the validity of using angular ground radiances to estimate cloud height and emissivity can been proven, then these principles can be extended to other areas of research such as instrumentation and radiative cloud modelling.

REFERENCES

Air Force Cambridge Research Laboratories, 1965: Handbook of Geophysics and Space Environments. McGraw-Hill, New York.

Allen, J. R., 1970: Measurements of cloud emissivity in the 8-13 μ waveband. J. Appl. Meteor., 10, 260-265.

Bignell, K. S., 1970: The water vapor infrared continuum. Q. J. Royal Meteor. Soc., 96, 390-403.

Coulson, K., 1975: Solar and Terrestrial Radiation. Academic Press, Inc., New York, 322 pp.

Cox, S. K., 1971: Cirrus clouds and the climate. J. Atmos. Sci., 28, 1513-1515.

Cox, S. K., 1975: Observations of cloud infrared effective emissivity. J. Atmos. Sci., 33, 287-289.

Cox, S. K., M. Polifka, K. Griffith, A. Rockwood, D. Starr, 1976: Radiative transfer computational routines for atmospheric science applications. Atmospheric Science Research Report, Colorado State University, 75 pp.

Davies, J. A., M. Abdel-Wahab, J. E. Howard, 1985: Cloud transmissivities for Canada. Mon. Wea. Rev., 113, 338-348.

Fleming, J., and S. K. Cox, 1974: Radiative effects of cirrus clouds. J. Atmos. Sci., 31, 2182-2188.

Griffith, K. T., S. K. Cox, R. G. Knollenberg, 1979: Infrared radiative properties of tropical cirrus clouds inferred from aircraft measurements. J. Atmos. Sci., 37, 1077-1087.

Liou, K. N., 1980: An Introduction to Atmospheric Radiation. Academic Press, Inc., Orlando, 392. pp.

McClatchey, R. A., et al., 1972: Optical properties of the atmosphere, (third edition). Air Force Cambridge Research Laboratories, Environmental Research Papers, No. 411, 108 pp.

Minitab: Data Analysis Software. Pennsylvania State University, State College, PA.

Paltridge, G. W., 1974: Infrared emissivity, Short-wave albedo, and the microphysics of stratiform water clouds. J. Geophy. Res., 79, 4053-4058.

Platt, C. M. R., 1973: Lidar and radiometric observations of cirrus clouds. J. Atmos. Sci., 30, 1191-1204.

Platt, C. M. R., 1974: Infrared emissivity of cirrus-simultaneous satellite, lidar and radiometric observations. Q. J. R. Met. Soc., 101, 119-126.

Shenh, W. E., R. J. Curran, 1973: A multi-spectral method for estimating cirrus cloud top heights. J. Appl. Meteor., 12, 1213-1216.

Smith, W. L., 1970: Iterative solution of the radiative transfer equation for the temperature and absorbing gas profile of an atmopshere. Appl. Optics, 9, 1993-1999.

Stamm, A. J., T. H. Vonder Haar, 1970: Atmospheric Effects on Remote Sounding. Univ. of Wisconsin, Madison. Project #100823.

Stephens, G. L., 1984: Cloud decoupling of the surface and planetary radiative budgets. J. Atmos. Sci., 41, 681-686.

Wallace, J. M., P. V. Hobbs, 1977: Atmospheric Science. Academic Press, London, 467 pp.

Yamamoto, G., M. Tanaka, S. Asano, 1969: Radiative transfer in water clouds in the infrared region. J. Atmos. Sci., 27, 282-292.

Zdunkowski, W. G., W. K. Crandall, 1971: Radiative transfer of infrared radiation in model clouds. Tellus, 23, 517-526.

END

DATE

FILMED

DEC.

1987